Author/s:
Beasley, JT;Bonneau, JP;Moreno-Moyano, LT;Callahan, DL;Howell, KS;Tako, E;Taylor, J;Glahn, RP;Appels, R;Johnson, AAT

Title:
Multi-year field evaluation of nicotianamine biofortified bread wheat

Date:
2022-03-01

Citation:
Beasley, J. T., Bonneau, J. P., Moreno-Moyano, L. T., Callahan, D. L., Howell, K. S., Tako, E., Taylor, J., Glahn, R. P., Appels, R. & Johnson, A. A. T. (2022). Multi-year field evaluation of nicotianamine biofortified bread wheat. Plant Journal, 109 (5), pp.1168-1182. https://doi.org/10.1111/tpj.15623.

Multi-year field evaluation of nicotianamine biofortified bread wheat

Jesse T. Beasley[a], Julien P. Bonneau[a], Laura T. Moreno-Moyano[a], Damien L. Callahan[b], Kate S. Howell[c], Elad Tako[d], Julian Taylor[e], Raymond P. Glahn[f], Rudi Appels[c], Alexander A. T. Johnson[a*]

[a]School of BioSciences, The University of Melbourne, Victoria 3010, Australia
[b]School of Life and Environmental Sciences, Deakin University, Victoria 3125, Australia
[c]School of Agriculture and Food, The University of Melbourne, Victoria 3010, Australia
[d]Department of Food Science, Cornell University, Stocking Hall, Ithaca, NY, 14853-7201, USA
[e]School of Agriculture, Food and Wine, University of Adelaide, Glen Osmond, South Australia 5064, Australia
[f]Robert W. Holley Center for Agriculture and Health, USDA-ARS, Ithaca, New York 14853, USA

*Correspondence: Tel.: + 61 3 8344 3969, E.: johnsa@unimelb.edu.au

Running title

Field evaluation of NA biofortified bread wheat

Keywords

Biofortification, Bioavailability, White flour, Bread, Confined field trials, Multi-environment, Nutrition, Anaemia, Hidden hunger, *Triticum aestivum* L.

Abstract

Conventional breeding efforts for iron (Fe) and zinc (Zn) biofortification of bread wheat (*Triticum aestivum* L.) have been hindered by a lack of genetic variation for these traits and negative correlation between grain Fe and Zn concentrations and yield. We have employed genetic engineering to constitutively express (CE) the rice nicotianamine synthase 2 (*OsNAS2*) gene and upregulate biosynthesis of two metal chelators – nicotianamine (NA) and 2'-deoxymugineic acid (DMA) – in bread wheat, resulting in increased Fe and Zn concentrations in wholemeal and white flour. Here we describe multi-location confined field trial (CFT) evaluation of a low-copy transgenic CE-*OsNAS2* wheat event (CE-1) over three years and demonstrate higher concentrations of NA, DMA, Fe and Zn in CE-1 wholemeal flour, white flour and white bread, and higher Fe bioavailability in CE-1 white flour relative to a null segregant (NS) control. Multi-environment models of agronomic and grain nutrition traits revealed a negative correlation between grain yield and grain Fe, Zn, and total protein concentrations, yet no

correlation between grain yield and grain NA and DMA concentrations. White flour Fe bioavailability was positively correlated with white flour NA concentration, suggesting that NA-chelated Fe should be targeted in wheat Fe biofortification efforts.

Introduction

The two major types of wheat, bread wheat (*Triticum aestivum* L.) and durum wheat (*Triticum durum* L.), are produced on more land than any other crop and processed into a variety of foods such as bread, noodles and pasta to supply ~20% of daily calorie intake to humans[1,2]. Wheat production exceeded 770 million tons (MT) in 2017 and superseded rice (*Oryza sativa* L.) as the second most produced crop behind maize (*Zea mays* L.) in that year (FAOSTAT, http://www.fao.org/faostat). Within less developed countries of wheat primary production, such as countries in the MENAP (Middle East, North Africa, Afghanistan and Pakistan) region, wheat consumption can supply >40% of daily calorie intake and coincides with high prevalences of human iron (Fe) and zinc (Zn) deficiency[3,4]. Crop biofortification represents a sustainable strategy to increase human micronutrient intake[5], however, Fe and Zn biofortification of wheat has been hindered by a lack of genomic resources, significant genotype (G) x environment (E) effects and a negative association with grain yield under some environmental conditions[6–12].

International breeding efforts over the last two decades have developed elite disease resistant and high yielding biofortified wheat with increased grain Zn (up to 1.3-fold) by exploiting grain micronutrient variation in *Triticum dicoccoides* wild varieties and developing synthetic hexaploids[7,13,14]. Conventional breeding efforts to biofortify wheat with Fe have had limited success, with the largest increase in grain Fe (up to 1.2-fold) achieved by selecting for the functional allele of *NAM-B1* (commonly referred to as *Gpc-B1*) which encodes a transcription factor that regulates flag leaf senescence and the remobilization of Fe and Zn from leaf tissue to the grain[15–20]. Cereal biofortification through conventional breeding is also limited by the presence of dietary compounds such as phytate (inositol hexaphosphate), polyphenols and fibre that inhibit Fe and Zn absorption (bioavailability) in the human gut[21–24]. Most Fe and Zn (70-80%) in wheat grain colocalizes with phytate-containing globoids in outer grain tissues such as the aleurone layer of the endosperm, and increased Fe and Zn concentrations in wholemeal flour per se may therefore not improve dietary micronutrient absorption among wheat consuming populations[25–29]. The limited Fe and Zn (20-30%) in wheat inner endosperm does not colocalize with phytate and therefore has the potential to be more bioavailable, and modern plant biotechnology allows researchers to overcome the physiological barriers to endosperm loading and increase the concentrations of Fe and Zn in white flour[30]. Using genetic

modification (GM) to improve crop nutritional quality and/or processing traits was recently coined second-generation GM with great potential to benefit human health in less developed countries[31].

The loading of Fe and Zn into cereal grain is regulated by transporters and chelators with high metal specificity[27,32]. In wheat all Fe and Zn enters the grain via the phloem and into the crease, a grain region comprised of the vascular bundle and nucellar projection, prior to redistribution of Fe to the aleurone and Zn to embryo and crease tissues[26,28,33–36]. In the aleurone Fe is loaded and stored in cell vacuoles by vacuolar iron transporter (VIT) genes[37–39] and expression of the wheat *TaVIT2* gene under the control of an endosperm-specific high-molecular-weight glutenin promoter (HMW) redirects Fe from the aleurone into the endosperm, doubling white flour Fe concentration without increasing total grain Fe[27,40]. Phloem Fe is mostly bound to nicotianamine (NA), a non-protein amino acid that chelates Fe, Zn and other transition metals in higher plants and serves as a biosynthetic precursor to 2'-deoxymugenic acid (DMA), an endogenous Fe chelator in cereals that is secreted as a phytosiderophore to chelate Fe in the rhizosphere[41–45]. The majority of Fe in white wheat flour (representing the inner endosperm) is chelated to NA and/or DMA[46] and constitutive expression (CE) of the rice nicotianamine synthase 2 (*OsNAS2*) gene increases both Fe (up to 2-fold) and Zn (up to 4-fold) concentrations in white flour[30,47]. Multi-location confined field trial (CFT) evaluation of transgenic biofortified wheat plants such as HMW-*TaVIT2* and CE-*OsNAS2* is necessary to determine whether increased grain nutrition is maintained under realistic farming conditions while maintaining agronomic performance[48].

We have developed biofortified CE-*OsNAS2* wheat that accumulates additional grain NA, DMA, Fe and Zn and demonstrates no apparent yield penalty under glasshouse and field conditions[30]. Here we comprehensively investigate agronomy and wholemeal flour, white flour and white bread nutrition in CE-*OsNAS2* wheat in multi-location CFTs over three consecutive seasons.

Results

Soil properties and environmental conditions varied between confined field environments

Three transgenic sibling lines of bread wheat cultivar (cv.) Bobwhite constitutively expressing the rice nicotianamine synthase 2 (*OsNAS2*) gene (Figure 1a) and derived from a double-insert transgenic event (hereafter referred to as CE-1.1, CE-1.2, CE-1.3) were grown alongside a null segregant control derived from the same event (hereafter referred to as NS). Mace, an elite Australian wheat cv. was included as a check. Replicated plots of all genotypes were evaluated in CFTs at three representative wheat growing environments in Australia: Glenthorne in South Australia, and Katanning and Merredin in Western Australia in 2015, 2016 and 2017 (Supplementary Figures 1, 2). Soil pH, soil conductivity (EC) and the

concentrations of soil macronutrients including ammonium (NH_4), nitrate (NO_3), phosphorus (P) potassium (K), sulfate (SO_4), and organic carbon (C) and soil micronutrients including aluminium (Al), calcium (Ca), magnesium (Mg), sodium (Na), copper (Cu), iron (Fe) manganese (Mn), zinc (Zn) and boron (B) at Glenthorne, Katanning and Merredin across the three field seasons are provided in Supplementary Table 1. Total rainfall across the three field seasons varied between 493 to 949 mm at Glenthorne, 291 to 504 mm at Katanning, and 284 to 517 mm at Merredin (Supplementary Figure 3). Merredin and Katanning have more temperate climates relative to Glenthorne with warmer temperatures in the summer months and cooler temperatures in the winter months. Daily temperatures (minimum/maximum) at Glenthorne varied from 12.6/21.8 °C in 2015, 12.7/21.4 °C in 2016, and 13.1/22.0 °C in 2017, at Katanning from 9.3/23.5 °C in 2015, 9.3/21.9 °C in 2016, and 9.5/22.9 °C in 2017, and at Merredin from 12.5/26.0 °C in 2015, 10.8/23.8 °C in 2016, and 12.0/25.9 °C in 2017 (Supplementary Figure 3). Significant G x E components between CFTs were detected for all agronomic performance, wholemeal flour nutrition, white flour nutrition or leaf nutrition traits (Supplementary Table 2). Across all CFTs, the Bobwhite genotypes had lower ($p < 0.05$) agronomic performance and higher wholemeal flour, white flour and bran nutrition relative to the check cv. Mace, apart from wholemeal and white flour K concentrations (Figures 1-3, Supplementary Tables 3-8).

Constitutive OsNAS2 expression had variable effects on agronomic performance and improved the nutritional composition of wholemeal flour, white flour and bran across multiple field environments

Glenthorne

Over three years of CFTs at Glenthorne (Figure 1b), soil pH varied from 7.1 – 7.6 and the concentrations of soil Fe and Zn varied from 4.5 – 32 mg/Kg (Figure 1c). Plant height (cm) was lower ($p < 0.05$) in all CE-1 sibling lines over three field seasons, and thousand grain weight was lower in CE-1.1 ($p \leq 0.001$) and CE-1.3 ($p < 0.05$) in 2017 relative to NS (Figure 1d-e). Grain yield (kg ha^{-1}) was lower ($p < 0.05$) in all CE-1 sibling lines relative to NS, apart from CE-1.3 in 2016 and CE-1.2 in 2017 (Figure 1f). Grain number (m^2) was lower ($p \leq 0.01$) in all CE-1 sibling lines in 2015, and grain number (m^2), tiller number (m^2) and harvest index (%) were lower ($p < 0.05$) in CE-1.1 in 2016 relative to NS (Supplementary Table 3). Wholemeal and white flour Fe concentrations were higher ($p \leq 0.01$) in CE-1.1 over three field seasons, and wholemeal Fe concentrations were higher ($p \leq 0.001$) in CE-1.2 and CE-1.3 in 2016 relative to NS (Figure 1g). Wholemeal and white flour Zn concentrations ($p < 0.05$), and nicotianamine (NA) and 2'-deoxymugineic acid (DMA) concentrations ($p \leq 0.01$) were higher in all CE-1 sibling lines over three field seasons relative to NS, apart from white flour DMA concentrations in CE-1.1 and CE-1.3 in 2015 (Figure 1h-j). Bran Fe concentrations were higher ($p \leq 0.01$) in all CE-1 sibling lines in 2016 and CE-1.1

in 2017, and bran Zn concentrations were higher ($p \leq 0.01$) in all CE-1 sibling lines over three field seasons relative to NS (Supplementary Table 4). Sibling line CE-1.1 had higher ($p \leq 0.01$) wholemeal flour P concentrations in 2016, white flour P and total protein concentrations in 2015 and 2016, and wholemeal flour total protein concentrations across three field seasons relative to NS (Supplementary Table 5). In 2016, wholemeal Cu, Mg, Mn and S concentrations, white flour S concentrations, and bran Cu and S concentrations were higher ($p < 0.05$) in all CE-1 sibling lines relative to NS (Supplementary Tables 6-8).

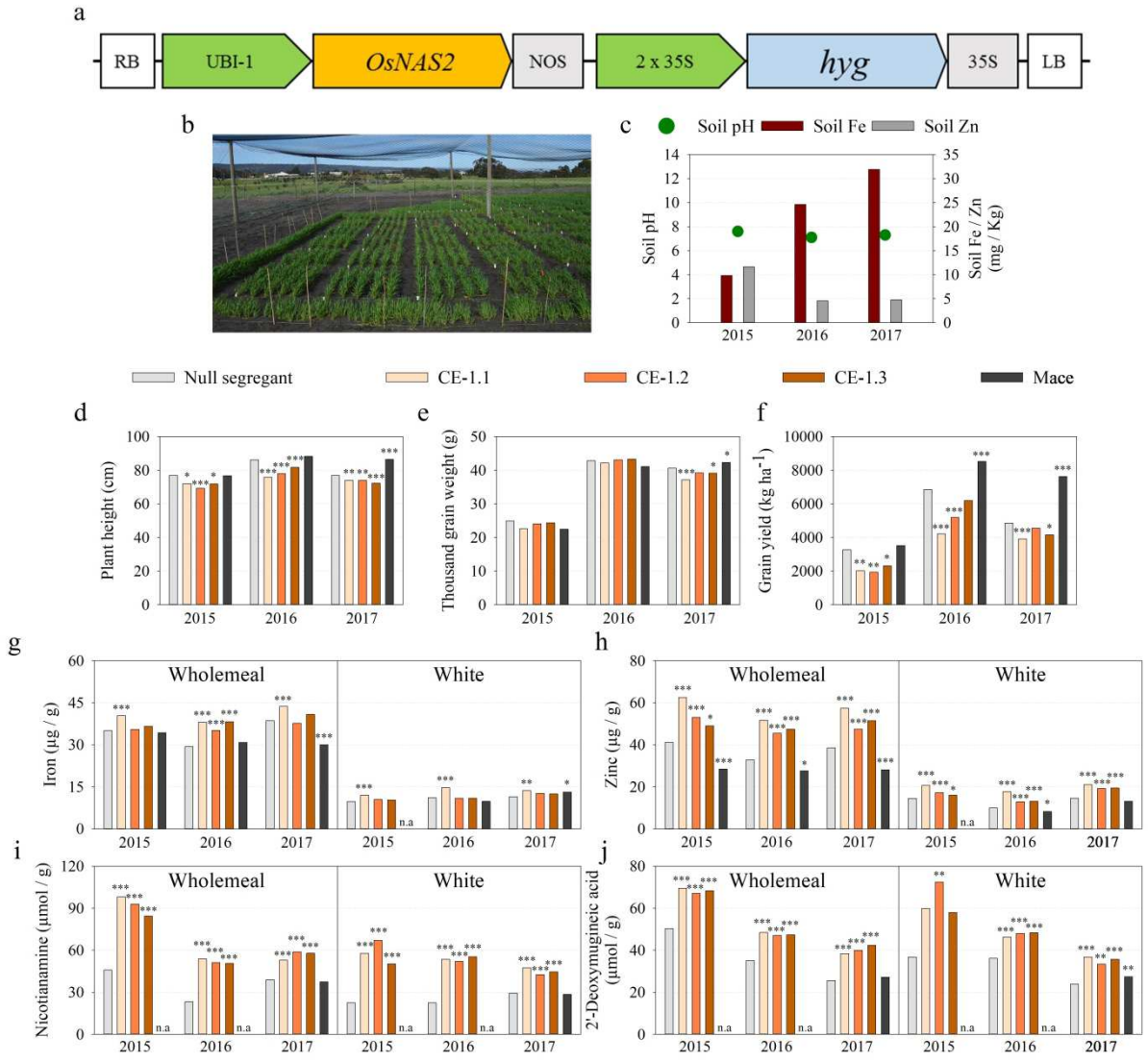

Figure 1. Agronomic performance of bread wheat constitutively expressing the rice nicotianamine synthase 2 (*OsNAS2*) gene (CE-1.1, CE-1.2, and CE-1.3) alongside the null segregant and cv. Mace over three field seasons at Glenthorne. **a**) Schematic representation of the T-DNA construct. RB and LB: right and left borders, respectively; UBI-1: maize ubiquitin 1 promoter; *OsNAS2*: rice nicotianamine synthase 2

gene (LOC_Os03 g19420); NOS: nopaline synthase terminator; 2 x 35S: dual promoter of 35S cauliflower mosaic virus gene; hyg: hygromycin phosphotransferase gene; 35S: terminator of 35S cauliflower mosaic virus gene. **b**) an image of replicated plots at Glenthorne during the 2017 field season. **c**) Soil pH (green circles), as well as soil Fe (red bars) and Zn (dark grey bars) concentrations (mg / Kg) are provided for the three field seasons. **d-j**) Bars indicate best linear unbiased estimators of the null segregant (light grey), CE-1.1 (light brown), CE-1.2 (orange), CE-1.3 (dark brown), and Mace (black) for **d**) plant height (cm), **e**) thousand grain weight (g), **f**) grain yield (kg ha^{-1}) and the concentrations of **g**) Fe (µg / g), **h**) Zn (µg / g), **i**) NA (µmol / g), and **j**) DMA (µmol / g) in wholemeal flour (left panel) and white flour (right panel). A minimum of three replicates per genotype were included for each field season and asterisks represent significant differences to the NS for $p < 0.05$ (*), $p \leq 0.01$ (**), $p \leq 0.001$ (***) as determined by Wald test. n.a = not applicable.

Katanning

Over three years of CFTs at Katanning (Figure 2a), soil pH varied between 4.4 – 5.3, soil Fe concentrations varied between 41.5 – 85.6 mg/Kg, and soil Zn concentrations varied between 1.4 – 13.6 mg/Kg (Figure 2b). Plant height (cm) and grain yield (kg ha^{-1}) were lower ($p < 0.05$) in CE-1.1 and CE-1.2 in 2015, and plant height (cm) was lower ($p \leq 0.01$) in all CE-1 sibling lines in 2016 relative to NS (Figure 2c-e). Tiller number (m^2), harvest index (%), biomass (kg ha^{-1}) and grain number (m^2) were lower ($p < 0.05$) in CE-1.1 and CE-1.2 in 2015 relative to NS (Supplementary Table 3). Wholemeal and white flour Fe, Zn, NA and DMA concentrations were higher ($p < 0.05$) in all CE-1 sibling lines over three field seasons relative to NS, apart from wholemeal flour Fe and Zn in CE-1.2 in 2015, white flour Fe in CE-1.2 in 2017, and wholemeal flour Zn in CE-1.3 in 2015 and CE-1.2 in 2016 (Figure 2f-i). Bran Fe concentrations were higher in CE-1.1 ($p \leq 0.001$) in 2015, CE-1.1 and CE-1.3 ($p \leq 0.01$) in 2016 and all CE-1 sibling lines ($p < 0.05$) in 2017 relative to NS (Supplementary Table 4). Bran Zn concentrations were higher ($p < 0.05$) in all CE-1 sibling lines over three field seasons relative to NS, apart from CE-1.2 and CE-1.3 in 2015. Sibling line CE-1.1 had higher ($p < 0.05$) wholemeal flour P concentrations in 2016 and 2017 and white flour P concentrations in 2015, and sibling line CE-1.3 had higher ($p < 0.05$) white flour P concentrations in 2015 and 2017 relative to NS (Supplementary Table 5). All CE-1 sibling lines had higher ($p \leq 0.01$) white flour total protein and S concentrations in 2015, white flour Ca concentrations in 2016, and white flour Mg concentrations over three field seasons relative to NS (Supplementary Tables 5, 7).

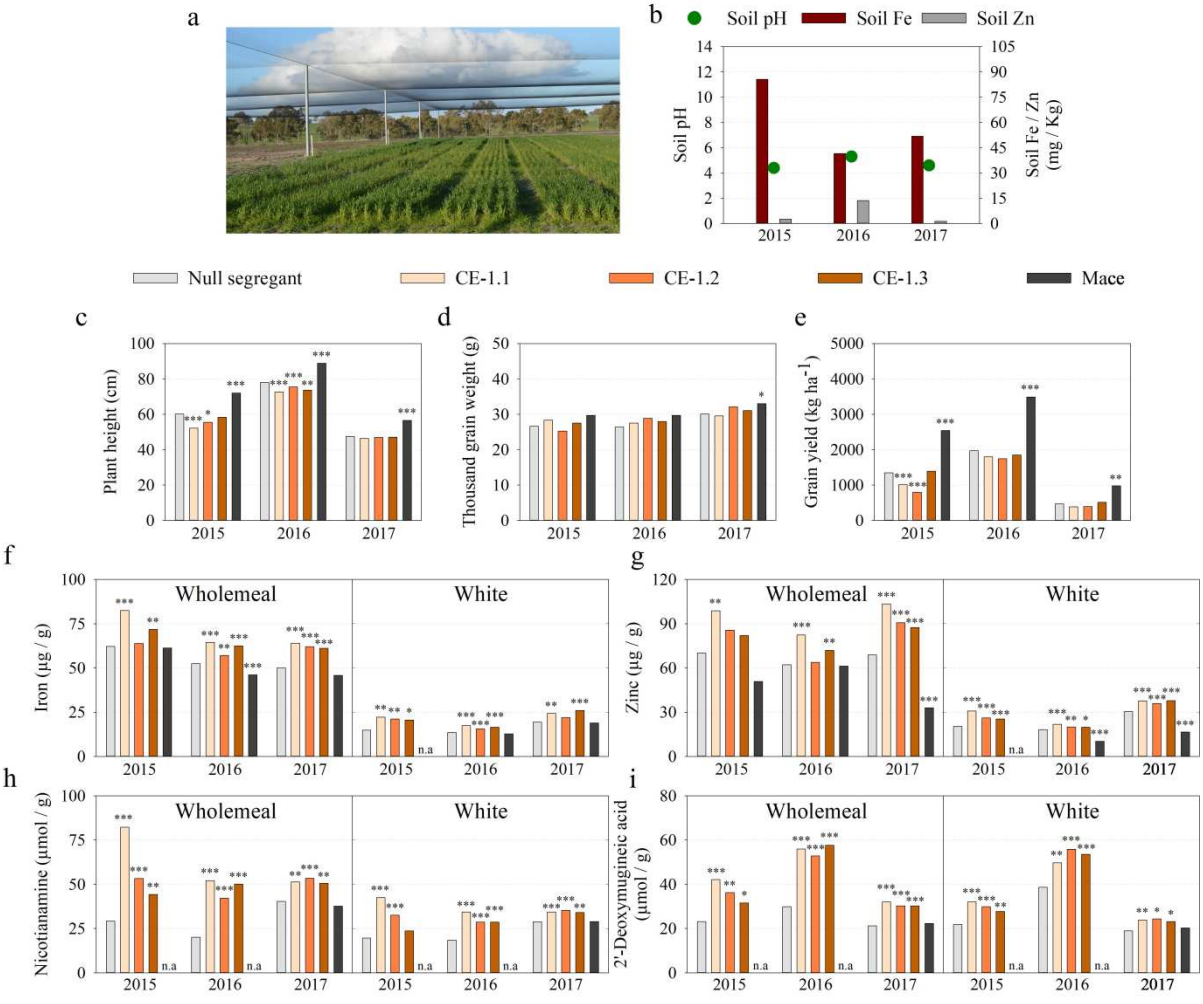

Figure 2. Agronomic performance, wholemeal and white flour nutritional composition of null segregant, CE-1.1, CE-1.2, CE-1.3 and Mace over three field seasons at Katanning. **a**) An image of 18m^2 replicated plots for the 2017 field season is provided. **b**) Soil pH (green circles), as well as soil Fe (red bars) and Zn (dark grey bars) concentrations (mg / Kg) are provided for the three field seasons. **c-i**) Bars indicate best linear unbiased estimators of the null segregant (light grey), CE-1.1 (light brown), CE-1.2 (orange), CE-1.3 (dark brown), and Mace (black) for **c**) plant height (cm), **d**) thousand grain weight (g), **e**) grain yield (kg ha^{-1}) and the concentrations of **f**) Fe (µg / g), **g**) Zn (µg / g), **h**) NA (µmol / g), and **i**) DMA (µmol / g) in wholemeal flour (left panel) and white flour (right panel). A minimum of three replicates per genotype were included for each field season and asterisks represent significant differences to the NS for $p < 0.05$ (*), $p \leq 0.01$ (**), $p \leq 0.001$ (***) as determined by Wald test. n.a = not applicable.

Merredin

Over three years of CFTs at Merredin (Figure 3a), soil pH varied between 4.6 – 4.8, soil Fe concentrations varied between 51.0 – 124.0 mg/Kg, and soil Zn concentrations varied between 1.4 – 2.3 mg/Kg (Figure 3b). Plant height (cm) and thousand grain weight were lower ($p \leq 0.01$) in CE-1.1 in 2016, plant height (cm) was lower ($p < 0.05$) in all CE-1 sibling lines in 2017, and grain yield (kg ha^{-1}) was lower ($p \leq 0.01$) in CE-1.1 in 2017 relative to NS (Figure 3c-e). Tiller number (m^2) was lower ($p < 0.05$) in CE-1.2 in 2015, biomass (kg ha^{-1}) was lower ($p \leq 0.01$) in CE-1.1 in 2016 and harvest index (%) was lower ($p < 0.05$) in CE-1.1 in 2017 relative to NS (Supplementary Table 3). Wholemeal flour Fe concentrations were higher ($p \leq 0.001$) in CE-1.1 in 2015, and wholemeal flour Fe and Zn concentrations were higher ($p < 0.05$) in CE-1.1 and CE-1.2 in 2016 and all CE-1 sibling lines in 2017 relative to NS (Figure 3f-g). White flour Fe concentrations were higher ($p \leq 0.01$) in CE-1.1 in 2015 and 2016, and white flour Zn concentrations were higher ($p \leq 0.001$) in all CE-1 sibling lines in 2016 and CE-1.1 in 2017 relative to NS. Wholemeal and white flour NA and DMA concentrations were higher ($p < 0.05$) in all CE-1 sibling lines over three field seasons relative to NS, apart from white flour DMA concentrations in CE-1.3 in 2016 (Figure 3h-i). Bran Fe concentrations were higher in CE-1.1 ($p \leq 0.001$) in 2015 and CE-1.3 ($p < 0.05$) in 2016 relative to NS (Supplementary Table 4). Bran Zn concentrations were higher ($p < 0.05$) in CE-1.1 over three field seasons and CE-1.3 in 2017 relative to NS. Sibling line CE-1.1 had higher ($p < 0.05$) wholemeal flour P and Mn concentrations in 2016 and 2017, total protein concentrations in 2015 and 2016, and Mg and S concentrations over three field seasons relative to NS (Supplementary Tables 5, 6). All CE-1 sibling lines had higher ($p < 0.05$) white flour Cu concentrations in 2016, white flour Mg concentrations in 2015 and 2017, white flour S concentrations in 2015 and 2016 relative to NS (Supplementary Tables 5, 7). All CE-1 sibling lines had lower ($p < 0.05$) bran Mg concentrations in 2016 relative to NS (Supplementary Table 8).

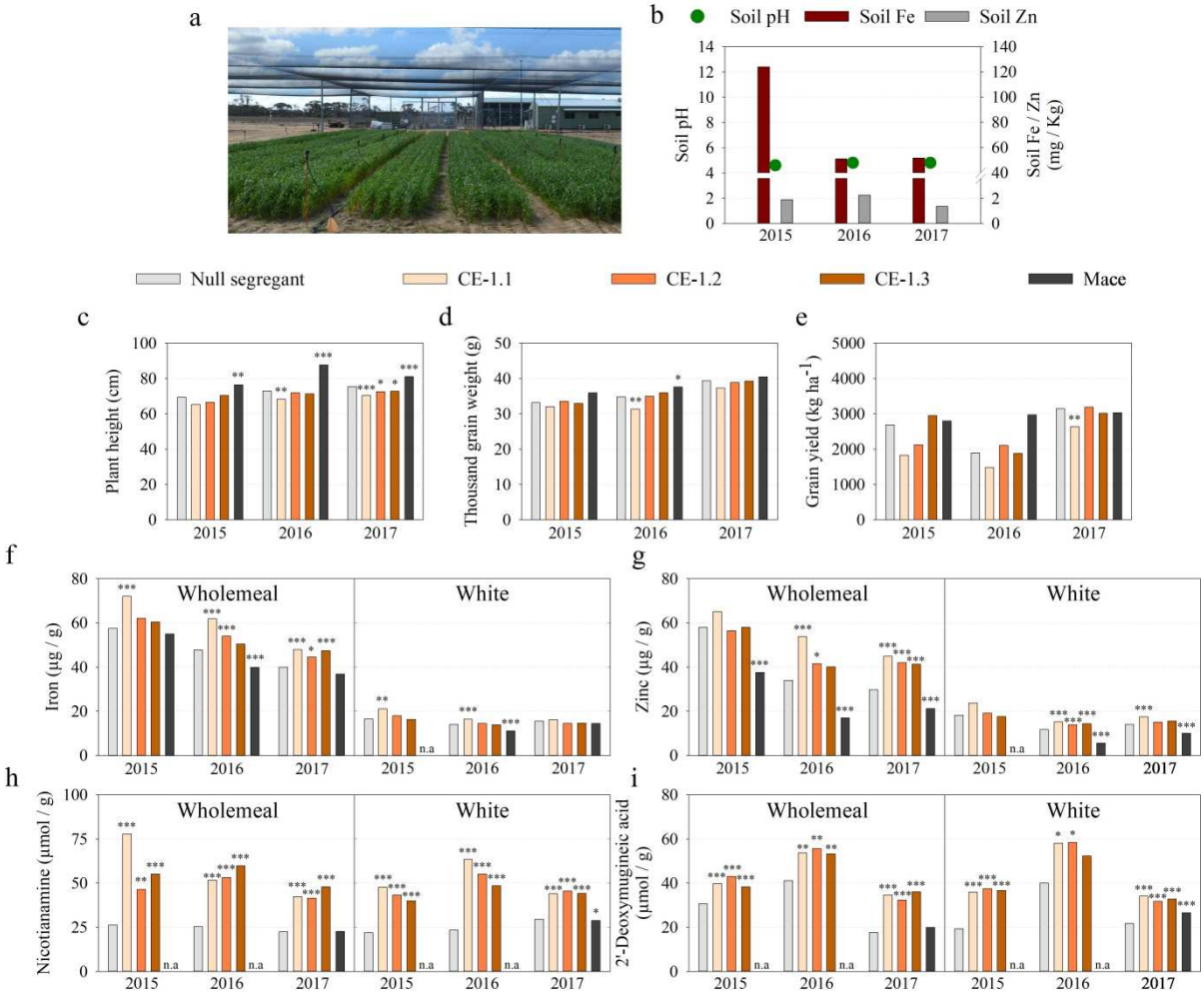

Figure 3. Agronomic performance, wholemeal and white flour nutritional composition of null segregant, CE-1.1, CE-1.2, CE-1.3 and Mace over three field seasons at Merredin. **a**) An image of 18m^2 replicated plots for the 2017 field season is provided. **b**) Soil pH (green circles), as well as soil Fe (red bars) and Zn (dark grey bars) concentrations (mg / Kg) are provided for the three field seasons. **c-i**) Bars indicate best linear unbiased estimators of the null segregant (light grey), CE-1.1 (light brown), CE-1.2 (orange), CE-1.3 (dark brown), and Mace (black) for **c**) plant height (cm), **d**) thousand grain weight (g), **e**) grain yield (kg ha^{-1}) and the concentrations of **f**) Fe (µg / g), **g**) Zn (µg / g), **h**) NA (µmol / g), and **i**) DMA (µmol / g) in wholemeal flour (left panel) and white flour (right panel). A minimum of three replicates per genotype were included for each field season and asterisks represent significant differences to the NS for $p < 0.05$ (*), $p \leq 0.01$ (**), $p \leq 0.001$ (***) as determined by Wald test. n.a = not applicable.

Constitutive OsNAS2 expression had variable effects on leaf nutrition across multiple environments

Flag leaf Fe concentrations were lower ($p < 0.05$) in CE-1.1 at Katanning in 2016 and Merredin in 2015, in CE-1.2 at Katanning in 2015 and Merredin over three field seasons, and in CE-1.3 in Katanning and Merredin in 2016 (Supplementary Table 9). All CE-1 sibling lines had higher ($p < 0.05$) flag leaf P concentrations at Glenthorne in 2016 and Merredin in 2015, higher ($p \leq 0.01$) flag leaf K concentrations at Glenthorne in 2016 and Merredin in 2017, and higher ($p < 0.05$) flag leaf and leaf S concentrations at Merredin in 2015 relative to NS (Supplementary Tables 9-11). Leaf Fe and S were negatively correlated with leaf P ($r < -0.80$, $p < 0.01$) and leaf Fe was negatively correlated with flag leaf Zn ($r < -0.80$, $p < 0.05$) (Supplementary Figure 4). Leaf Cu and K were positively correlated ($r > 0.90$, $p \leq 0.001$) and negatively correlated with leaf Ca ($r < -0.90$, $p \leq 0.001$), Mg, Mn, and P ($r < -0.70$, $p < 0.05$). Flag leaf removal at anthesis did not affect the concentration of grain Fe in CE-1.2, CE-1.3 and NS at Katanning, yet in the glasshouse, flag leaf removal reduced grain Fe concentrations in CE-1.2 and CE-1.3 and not NS (Supplementary Figure 5). Flag leaf removal at anthesis resulted in a higher ($p \leq 0.01$) concentration of grain Zn in CE-1.2 and CE-1.3 relative to NS at Katanning.

White flour Fe bioavailability was positively correlated with grain NA and DMA concentrations and grain yield, and negatively correlated with grain Fe, Zn, P and protein concentrations

Iron bioavailability determined through the coupled *in vitro* digestion/Caco-2 cell model was higher ($p < 0.05$) in white flour of all CE-1 sibling lines at Glenthorne and Katanning in 2015, CE-1.3 at Glenthorne in 2016, CE-1.1 and CE-1.2 at Katanning in 2016, and CE-1.3 at Glenthorne and Katanning in 2017 relative to NS (Supplementary Figure 6). At Merredin, Fe bioavailability was higher ($p < 0.01$) in white flour of CE-1.2 relative to NS in 2015 and did not differ between Bobwhite genotypes in 2016 and 2017. Across all CFTs white flour Fe bioavailability was positively correlated with white flour NA concentration ($r = 0.77$, $p < 0.05$) (Figure 4). Wholemeal and white flour Fe, Zn and total protein concentrations were positively correlated ($r \geq 0.93$, $p \leq 0.001$), and negatively correlated with tiller number ($r \leq -0.75$, $p < 0.05$), plant height ($r < -0.95$, $p \leq 0.001$), plant biomass ($r \leq -0.86$, $p \leq 0.001$), grain number ($r \leq -0.93$, $p \leq 0.001$), and grain yield ($r \leq -0.92$, $p \leq 0.001$). All wholemeal and white flour nutrition traits clustered separately from agronomic performance traits except for wholemeal and white flour NA, DMA and Cu concentrations, white flour K concentrations and white flour Fe bioavailability (Supplementary Figure 7).

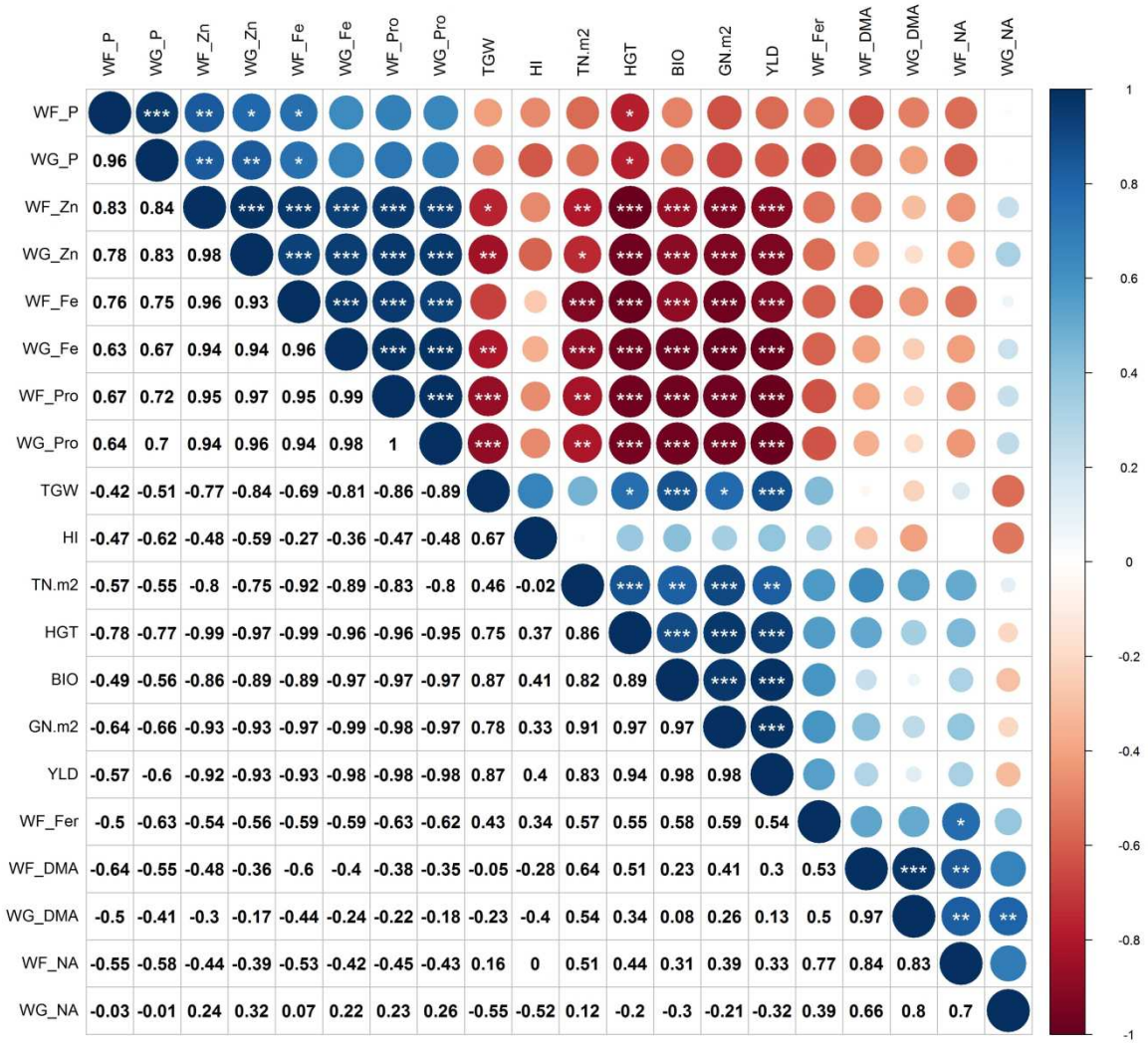

242

243 **Figure 4.** Multi-trait correlation of empirical best linear unbiased estimators (eBLUEs) obtained from the
244 multi-environment models of agronomic performance, grain nutrition and white flour nutrition of NS,
245 CE-1, and Mace over three field seasons at all locations. Agronomic performance variables include grain
246 yield (YLD), harvest index (HI), thousand grain weight (TGW), total biomass (BIO), tiller number per m^2
247 (TN.m2), grain number per m^2 (GN.m2), plant height (HGT). Wholemeal (WG) and white flour (WF)
248 nutrition variables include Fe, Zn, P, NA, and DMA concentrations, total protein (Pro) and Caco-2 cell
249 ferritin production (Fer). Each circle represents a positive (blue) or negative (red) pairwise Pearson
250 correlation coefficient between variables, with the diameter of the circle proportional to the absolute
251 value. Asterisks denote significant correlations for $p < 0.05$ (*), $p \leq 0.01$ (**), $p \leq 0.001$ (***).

252

Constitutive OsNAS2 expression improved grain fraction and white bread nutritional composition across multiple field environments

Iron, Zn, NA and DMA concentrations were higher ($p < 0.05$) in all CE-1 grain fractions relative to NS at Merredin in 2017, except for Fe and Zn in break 1 and 2 and Fe in reduction 1 (Table 1). Phytate concentrations were higher ($p < 0.05$) in break 3, reduction 2 and bran of CE-1 grain relative to NS, and in CE-1.3 white flour relative to the NS at Katanning in 2017 (Table 1, Supplementary Figure 8). White bread Fe, Zn, NA and DMA concentrations were higher ($p \leq 0.01$) in all CE-1 sibling lines relative to NS at all field locations in 2016, apart from Fe concentrations in all CE-1 sibling lines at Glenthorne (Figure 5a-d).

Table 1. The concentrations of Fe (µg / g), Zn (µg / g), NA (µmol / g), DMA (µmol / g), and phytate (mg / g) in null segregant (NS) and CE-1 grain fractions at Merredin in 2017. Values represent mean ± SEM of three biological replicates with three technical replicates for Fe and Zn, four biological replicates for NA and DMA, and two biological replicates with three technical replicates for phytate. Asterisks denote significant differences for $p < 0.05$ (*), $p \leq 0.01$ (**), $p \leq 0.001$ (***) as determined by Student's t-test.

Grain Region	Fraction	Iron (µg / g)	Zinc (µg / g)	Nicotianamine (µmol / g)	2'-Deoxymugineic Acid (µmol / g)	Phytate (mg / g)
Endosperm	NS Break 1	17.9 ± 0.4	11.4 ± 0.1	33.9 ± 0.1	25.8 ± 0.3	1.3 ± <0.1
	CE-1 Break 1	19.5 ± 0.7	13.2 ± 0.6	50.6 ± 1.1***	35.5 ± 0.8***	1.4 ± <0.1
	NS Break 2	19.3 ± <0.1	11.6 ± 0.1	34 ± 0.2	25.2 ± 0.7	1.2 ± 0.1
	CE-1 Break 2	22 ± 0.9	12.4 ± 0.2	51.5 ± 0.7***	34.5 ± 0.6***	1.2 ± <0.1
	NS Break 3	37.8 ± 1.4	16.8 ± 0.4	33.7 ± 0.1	25 ± 0.2	2.8 ± <0.1
	CE-1 Break 3	45.8 ± 0.8*	22.6 ± 0.2***	51 ± 0.4***	36.8 ± 1.3***	3.3 ± <0.1*
	NS Reduction 1	13.8 ± 0.3	12.1 ± 0.1	33.9 ± 0.3	25.6 ± 0.3	1.5 ± <0.1
	CE-1 Reduction 1	16.1 ± 1.1	14.3 ± 0.1***	53.2 ± 0.2***	36.6 ± 0.7***	1.7 ± 0.1
	NS Reduction 2	18.6 ± 0.1	16.6 ± 0.1	35.9 ± 0.3	27.5 ± 0.6	1.9 ± <0.1
	CE-1 Reduction 2	24.9 ± 0.1**	24 ± 0.2***	52.7 ± 0.7***	35.9 ± 0.4***	2.5 ± <0.1***
	NS Reduction 3	30 ± 0.6	25.3 ± <0.1	35.8 ± 0.5	25.4 ± 0.7	3.4 ± 0.2
	CE-1 Reduction 3	35.5 ± 0.4***	33.3 ± 0.2***	53.4 ± 0.3***	36.3 ± 1.3***	3.2 ± 0.1
Aleurone	NS Pollard	107.3 ± 1.1	84.6 ± 0.9	45.3 ± 0.4	25.9 ± 0.2	9.4 ± 0.3
	CE-1 Pollard	123.2 ± 0.9***	102.1 ± 0.7***	69.7 ± 0.4***	34.7 ± 0.4***	7.6 ± 0.2
Pericarp / Testa	NS Bran	135.2 ± 0.4	95.7 ± 0.4	50.2 ± 0.7	27.4 ± 0.4	10.4 ± 0.2
	CE-1 Bran	148.2 ± 1.5***	115.5 ± 0.5***	71.5 ± 0.7***	34.8 ± 0.5***	13.8 ± 0.5*

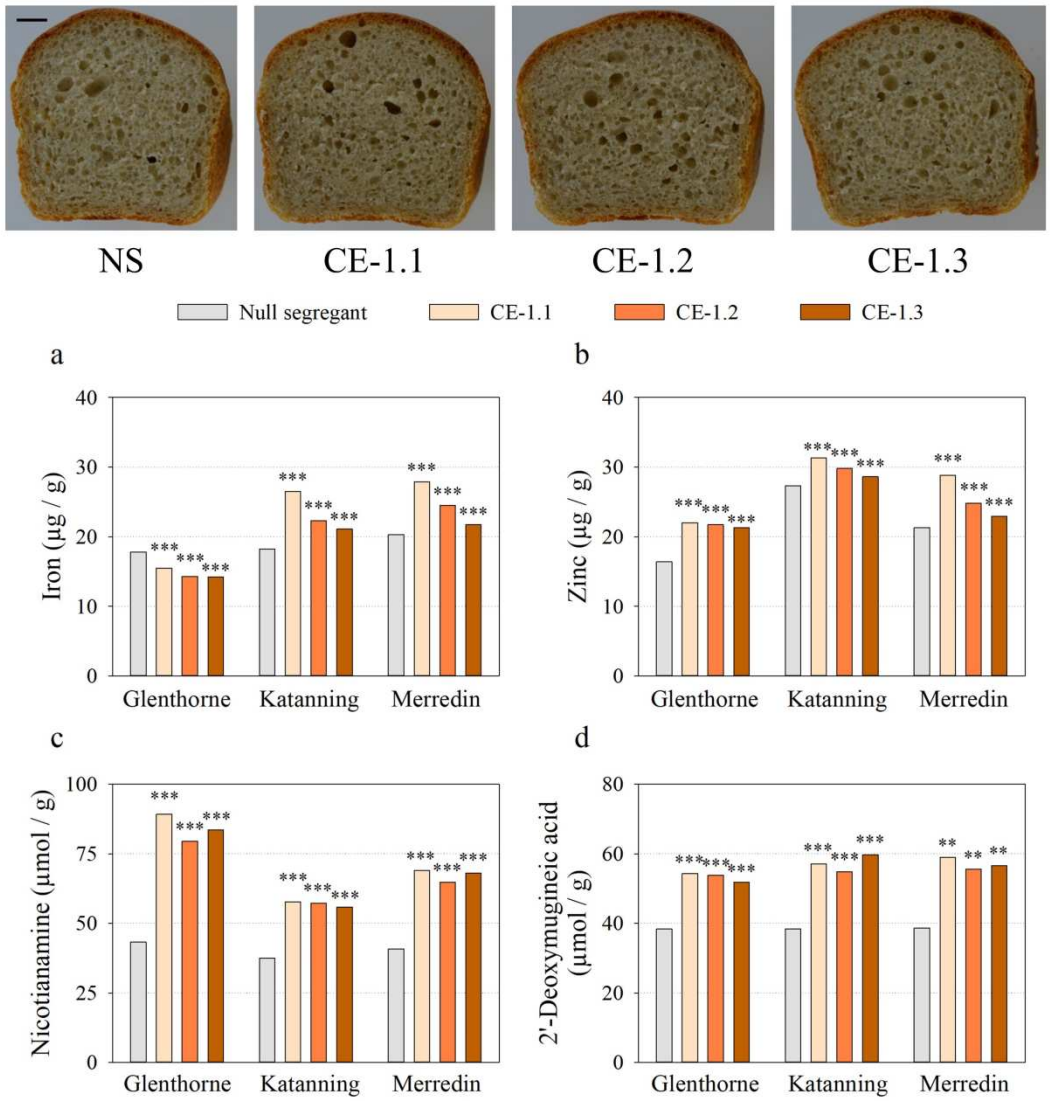

Figure 5. White bread nutritional composition of NS and CE-1 sibling lines at Glenthorne, Katanning and Merredin. Bars indicate best linear unbiased estimators for the concentrations of **a**) Fe (µg / g), **b**) Zn (µg / g), **c**) NA (µmol / g), and **d**) DMA (µmol / g) at each field site in 2016. Three replicates per genotype were included in the analysis and asterisks represent significant differences to the NS for $p < 0.05$ (*), $p \leq 0.01$ (**), $p \leq 0.001$ (***) as determined by Wald test. Photos show representative cross sections of NS and CE-1 loaves from Katanning prior to analysis. Scale bar = 1cm.

Discussion

A key component of biofortified crop development involves multi-location CFTs to determine if target micronutrient concentrations are affected by genotype x environment (G x E) interactions and/or have impacts on yield[5,49]. Previous field evaluation of Zn biofortified wheat cultivars at nine different locations highlighted significant G x E interactions on grain Fe and Zn concentrations, and confirmed that grain nutrition was more affected by environment than genotype[15]. More recent multi-location CFT evaluation of two leading Fe and Zn biofortified rice transgenic events overexpressing the *OsNAS2* gene in combination with endosperm-specific expression of the soybean (*Glycine max* L.) ferritin *(Sfer-H1)* gene uncovered that one event (termed NASFer-274) exhibited no yield penalty relative to the null control[48]. We previously reported that CE-1 wheat plants exhibited no apparent agronomic difference to NS plants when grown under glasshouse and field conditions, however, the field component of that research was limited to two sites and one season[30]. In this study we comprehensively evaluated three CE-1 sibling lines in multi-location CFTs over three field seasons and detected a small but consistently significant reduction in plant height for all three CE-1 sibling lines relative to NS (Figures 1-3). Increased *NAS* gene activity may reduce plant height through altered biosynthesis of the phytohormone ethylene, given that S-adenosyl methionine (SAM) is the biosynthetic precursor to both ethylene and NA, and ethylene plays fundamental roles in leaf development, senescence and fruit ripening[50]. Modifying ethylene biosynthesis and the downstream targets of ethylene improves crop yield and abiotic stress tolerance in corn (*Zea mays*, L.) and rice[51,52] and determining whether altered ethylene biosynthesis is responsible for the reduced plant height in CE-1 sibling lines warrants further investigation. Nevertheless, the slight reduction in plant height observed in all three CE-1 sibling lines could be advantageous by helping to prevent lodging. Variability in agronomic performance, wholemeal flour nutrition and white flour nutrition (Figures 1-3 and Supplementary Tables 3, 5-7) between CE-1 sibling lines is likely due to somaclonal variation[53] and backcrossing of CE-1 lines to wild-type wheat will be required to remove this variation prior to dissemination. Similar findings were documented during field trial evaluation of barley (*Hordeum vulgare* L.), where agronomic performance varied between sibling lines of the same transgenic event at the second (T_2) and fourth (T_4) generations[54]. Together these results suggest that CFT evaluation of transgenic plants should occur over multiple generations and utilize multiple sibling lines per transgenic event. Importantly although we detected significant G x E components in our study (Supplementary Table 2), between field sites all CE-1 sibling lines exhibited similar agronomic performance and grain nutrition relative to the NS suggesting that CE-*OsNAS2* exhibits the same effect regardless of field condition.

Plant Fe is mostly stored as phytoferritin in leaf tissues and during grain filling metal chelators such as NA and/or DMA facilitate long-distance remobilization of Fe from leaf tissues to the developing

grain[41,55]. To determine the proportion of Fe and Zn that is remobilized from CE-1 and NS leaves to the grain during grain filling, we removed flag leaves and leaves from CE-1 and NS plants at anthesis when grown in the glasshouse (soil pH ~ 6.0) and at Katanning (soil pH ~4.8). Flag leaf removal reduced grain Fe and Zn concentrations in CE-1 plants more than in NS plants when grown in the glasshouse but not at Katanning, suggesting that soil pH influences the remobilization of micronutrients from CE-1 leaves to the developing grain (Supplementary Figure 5). We hypothesize that under glasshouse conditions of higher soil pH, CE-1 plants remobilize a greater proportion of leaf Fe and Zn to the developing grain, as higher soil pH limits the availability of soil Fe and Zn for plant uptake[56,57]. By contrast, the lower soil pH at Katanning increases the availability of soil Fe and Zn (Figure 1c, Supplementary Table 1) and may therefore allow more direct remobilization from below ground sources to the grain during CE-1 grain filling. Furthermore, soil micronutrient concentrations varied between field locations and across seasons (for example, Katanning and Merredin soil Fe concentrations were between 1.7- to 2.4-fold higher in 2015 relative to 2016 and 2017) and likely influenced final grain Fe and Zn concentrations, further highlighting the importance of conducting multi-location CFTs across multiple generations (Figures 1-3). Mature CE-1 flag leaves contained lower ($p < 0.05$) Fe than NS leaves (Supplementary Table 9), suggesting that CE-1 plants remobilize additional Fe from leaf tissue to the grain during grain filling relative to NS plants. It is likely that this remobilization is mediated by increased NA concentrations in CE- leaves given that CE-1 shoots contain higher NA concentrations relative to NS shoots[30]. As NA chelates other micronutrients such as Cu and Mn[43], increased NA-mediated remobilization from CE-1 leaves could explain increased concentrations of Cu and Mn in wholemeal and white flour of CE-1 relative to NS (Supplementary Tables 6-8). Grain Cu concentrations were negatively correlated with all other grain nutrients (apart from white flour K) and positively correlated with agronomic performance traits, although whether or not breeding for higher grain NA-chelated Cu concentration may indirectly improve grain yield requires further investigation (Supplementary Figure 7). The positive correlation of white flour K with agronomic traits is likely the result of lower white flour K concentrations in Bobwhite relative to the check (Supplementary Table 7). Both NA and DMA are synthesized from S-adenosyl-methionine (a S-containing cosubstrate)[44], and upregulated biosynthesis of NA and/or DMA in CE-1 grain could explain the higher wholemeal and white flour S concentrations measured in all CE-1 sibling lines relative to the NS (Supplementary Tables 6, 7). Throughout our study we measured higher wholemeal and white flour Mg concentrations in all CE-1 sibling lines relative to NS, a result that was demonstrated in glasshouse grown wheat constitutively overexpressing *OsNAS2*[47], and suggests that NA may be capable of chelating and remobilizing Mg^{2+} ions. Future radioisotope and metabolomic studies are required to elucidate these hypothetical nutrient dynamics in CE-1 plants and to confirm the contribution of increased leaf NA and/or DMA concentrations to wheat grain nutrition[35].

At Glenthorne, Katanning and Merredin over three field seasons we measured significantly higher concentrations of Fe, Zn, NA and DMA in CE-1 wholemeal flour, and significantly higher concentrations of Zn, NA and DMA in CE-1 white flour relative to NS (Figures 1-3). White flour Fe concentrations were higher ($p < 0.05$) in all CE-1 sibling lines over three field seasons at Katanning (apart from CE-1.2 in 2017) yet were only higher ($p \leq 0.01$) in sibling line CE-1.1 at Glenthorne and Merredin. To further determine whether both Fe and Zn concentrations were higher throughout all CE-1 grain regions relative to NS, we performed industrial-scale milling (>30 kg per genotype) and obtained eight grain fractions: three break, three reduction, pollard, and bran, that represent the innermost and outermost grain layers (Table 1). We detected significantly higher Fe and Zn concentrations in CE-1 break, reduction, pollard (aleurone), and bran fractions relative to NS, providing strong evidence to suggest that Fe and Zn concentrations are higher throughout CE-1 grain (Table 1, Supplementary Table 4). Synchrotron X-ray fluorescence microscopy (XFM) analysis of glasshouse-grown CE-1 and NS grain demonstrated that CE-1 grain contained enhanced Fe and Zn in aleurone tissues and only an enhanced Fe signal in endosperm tissues[30]. Together these results indicate that break/reduction flour Fe and Zn concentrations measured in our study are most likely derived from endosperm and crease tissues, respectively that are retained during roller milling[58]. We detected significantly ($p \leq 0.001$) higher NA and DMA concentrations in all CE-1 grain fractions relative to NS, suggesting that constitutive *OsNAS2* expression increases NA and DMA throughout the wheat grain (Table 1). Increased NA and DMA concentrations in break and reduction fractions would likely increase Fe bioavailability given that these fractions contain low concentrations of phytate (< 3.5 mg/g) and that these chelators are strong enhancers of Fe bioavailability[59]. The high concentrations of phytate (> 7.0 mg/g) within CE-1 outer grain fractions would likely counteract the effect of increased NA and DMA concentrations on Fe bioavailability, given that *in vitro* analyses demonstrated no difference in CE-1 and NS wholemeal flour Fe bioavailability[30]. White flour Fe bioavailability was higher in all CE-1 sibling lines relative to the NS throughout our study and positively correlated with white flour NA and DMA concentrations (Figure 4, Supplementary Figures 6, 7). We have previously reported on improved white flour Fe bioavailability independent of Fe concentration[30] and similar results were observed in this study for sibling line CE-1.3 (Figure 1g, Supplementary Figure 6). These results provide additional evidence that NA and DMA are phytonutrients that strongly enhance Fe bioavailability in white flour and mediate the uptake of Fe into human cells[60,61]. In our study we demonstrate that wholemeal flour and white flour Fe and Zn concentrations were negatively correlated ($r \leq -0.92$, $p \leq 0.001$) with grain yield and uncover for the first time that white flour NA and DMA concentrations had a modest positive correlation ($r \geq 0.42$) with grain yield (Figure 4, Supplementary Figure 7). In some instances (e.g. Merredin, 2017) CE-1 sibling lines only had higher grain NA and DMA concentrations relative to the control, and may explain why grain yield was negatively correlated with

grain Fe, Zn and total protein concentrations and not with grain NA and DMA concentrations across all genotypes (Figure 4). Together these results suggest that a shift in focus towards breeding for increased grain NA and/or DMA concentrations could improve both grain Fe bioavailability without compromising agronomic performance within wheat biofortification programs.

Higher concentrations of Fe, NA, and DMA in CE-1 white bread relative to NS white bread at Katanning and Merredin, coupled with no difference in bread phytate/Fe ratios (Supplementary Figure 8), suggests that NA and DMA are thermostable and persist the breadmaking process and that CE-1 white bread will demonstrate enhanced Fe bioavailability (Figure 5). Given these findings, it is also worth investigating the effect of enhanced NA and DMA concentrations on wholemeal bread Fe bioavailability, given that wholemeal breads contain higher concentrations of Fe bioavailability inhibitors such as phytate, polyphenols and dietary fibre[21,24]. Due to a lack of *in vitro* screening tools we could not determine whether consistently higher concentrations of Zn in CE-1 wholemeal and white flour translates into higher Zn bioavailability. Future analysis of CE-1 flour and bread may therefore involve more comprehensive *in vivo* studies that have the capacity to simultaneously evaluate Fe and Zn bioavailability[62]. White bread Fe concentrations were higher in NS relative to CE-1 only at Glenthorne, suggesting that properties of the soil (particularly soil pH) indirectly influence white bread Fe nutrition (Figure 5a). The high soil pH at Glenthorne likely results in greater biosynthesis of NA and DMA in CE-1 plants relative to NS plants and higher molar ratios of NA/DMA to Fe[45]. We hypothesize that a greater proportion of NA and/or DMA-chelated Fe in CE-1 white bread relative to NS white bread at Glenthorne results in a lower proportion of Fe localised to the crumb relative to the crust (which was not sampled in this study). Furthermore, higher white flour S and total protein concentrations in CE-1 white flour relative to NS white flour (Supplementary Tables 5 and 7) likely affected dough rheology given that S and protein play important roles in the gluten complex, and may also contribute to altered Fe distribution in CE-1 white bread[63,64]. Future experiments will comprehensively determine the localization and speciation of Fe bound to NA and/or DMA within both the crumb and crust of CE-1 and NS white bread *via* synchrotron-based analyses[65]. Altogether our study further demonstrates the potential of NA biofortified, high-yielding wheat crops (such as CE-*OsNAS2*) for improving human micronutrient intakes in less developed countries.

Materials and methods

Generation of iron and zinc biofortified wheat

Vector construction, plant transformation and the initial selection of our lead transgenic event CE-1 is previously described[30]. In brief, the full-length coding sequence of *OsNAS2* (LOC_Os03g19420) was

PCR amplified from rice (*Orzya sativa* L.) cultivar (cv.) Nipponbare and recombined into a modified pMDC32 vector under transcriptional control of the maize (*Zea mays* L.) ubiquitin 1 promoter with a hygromycin phosphotransferase plant-selectable marker (Figure 1a). Bombardment of the construct into immature wheat (*Triticum aestivum* L.) cv. Bobwhite embryos was performed at the University of Adelaide (Adelaide, Australia) to generate six independent CE-*OsNAS2* transgenic events, and one double-insert event termed CE-1 was selected for additional analyses based on no difference in plant phenotype and increased grain Fe and Zn concentrations. Three sibling lines of CE-1 (termed CE-1.1, CE-1.2 and CE-1.3) and the corresponding null segregant control (NS) were selected for confined field trial (CFT) evaluation and were grown at the T_5, T_6 and T_7 generations consecutively alongside the check cv. Mace, an elite Australian bread wheat cultivar.

Confined field trials (CFTs)

Confined field trials were conducted from May to December in 2015, 2016 and 2017 at Glenthorne (35.0543° S, 138.5524° E) in South Australia and at the New Genes for New Environment facilities located in Merredin (31.4837°S, 118.2771°E) and Katanning (33.6894°S, 117.5551°E) in Western Australia. Grain were sown in 1 m^2 plots at Glenthorne across all three seasons and in 1.8 m^2 plots in 2015, 8.5 m^2 plots in 2016, and 18 m^2 plots in 2017 at Katanning and Merredin (Supplementary Figures 1, 2). At least three replicate plots per genotype were grown in 2015, five replicate NS and CE-1 sibling line plots and four replicate Mace plots were grown in 2016, and five replicate plots per genotype were grown in 2017. All plots were arranged in a randomized block design at each site. Rows were spaced 30 cm apart and grain were sown at a density of 60 kg ha^{-1} in 2015 and 2016, and 75 kg ha^{-1} in 2017 at all three sites. Fertilizers were applied as urea and/or AGRAS (CSBP limited, Kwinana, WA, Australia) at a rate of 40 – 100 kg ha^{-1} as needed for each field site. Leaves and flag leaves were harvested post-anthesis from each plot, cleaned with 0.1% Tween®20 (Sigma Aldrich, St. Louis, MO, USA), rinsed with dH_2O and oven dried for 48 h at 60°C before homogenization. At maturity, plant height and tiller number were determined from three representative measurements per plot and biomass, TGW, and harvest index were determined from subsamples of each plot as previously described[30]. Grain yield was calculated from the amount of grain harvested per m^2 and extrapolated to kg/ha. Soil analysis was performed at sowing at CSBP Soil and Plant Analysis Laboratory (Perth, WA, Australia). Soil phosphorus (P) and potassium (K) concentrations were determined using the Colwell P and K extraction methods[66,67]. A diethylenetriaminepentaacetic acid (DTPA) extraction method was used to calculate soil copper (Cu), iron (Fe), manganese (Mn), and zinc (Zn) concentrations[68]. Soil properties of each site for each season are shown in Supplementary Table 1 and field environmental conditions are shown in Supplementary Figure 3.

Analysis of iron and zinc remobilization post anthesis

Plants were grown under glasshouse conditions at The University of Melbourne (Victoria, Australia) as previously described[30]. At flowering, plants grown in the glasshouse and in the field at Katanning received one of three treatments: 1) all tillers apart from the main tiller removed (detillered), 2) detillered and main stem flag leaf removed (detillered - flag leaf), 3) detillered and all leaves removed (detillered - all leaves). Grain was harvested at maturity, cleaned, oven dried for 48 h at 60°C and ground into a powder. A subsample (20 mg) was digested with 300 µL aqua regia (1 HNO_3: 3 HCl) heated (80°C, 90 min), diluted to 10 mL with deionized H_2O (18 MΩ) and centrifuged (5,000 rpm, 5 min) prior to analysis by inductively coupled plasma mass spectrometry (ICP-MS) at Deakin University (Burwood, Australia)[69].

White flour and white bread production

Whole grain samples were conditioned to 13% moisture content for 24 h prior to milling using a Quadrumat Junior laboratory mill (Brabender, Duisburg, Germany) as previously described[30] and using a Buhler MLU-202 laboratory mill at The Commonwealth Scientific and Industrial Research Organisation (CSIRO, ACT, Australia) for grain fraction analysis of NS and a combined sample of CE-1.2 and CE-1.3 at Merredin, 2017. Flour extraction across all samples was between 70-75%. White bread was produced using a baker's yeast protocol as previously described[70] with minor modifications. White flour (500 g) was mixed with H_2O (325 g), 10 g of dry baker's yeast (Lowan® whole foods, NSW, Australia) and 10 g of cooking salt (Black & Gold, NSW, Australia) in a BM2500 Compact Bakehouse (Sunbeam, NSW, Australia) for 25 min, prior to fermentation for at least 1 hr. Dough was divided into 150 g pieces, shaped and placed into loaf tins (14.6 x 7.6 cm) for proofing (30 min, 30°C) and baking (20 min, 200°C) in a commercial oven (Convotherm 4 EasyDial 10.10, Moffat, VIC, Australia). Loaves were cooled (1 hr) before the crumb was separated from the crust as described in[71], lyophilized and ground to a powder for analysis.

Inductively coupled plasma optical emission spectrometry (ICP-OES)

Plant tissues were cleaned and ground using an IKA tube mill (www.ika.com) prior to inductively coupled plasma optical emission spectrometry (ICP-OES) analysis at the CSBP Soil and Plant Analysis Laboratory (Perth, WA, Australia) as previously described[30]. White flour and white bread micronutrient concentrations were determined by nitric / perchloric acid digestion as previously described[72] followed by ICP-OES using a Thermo iCAP 6500 series (Thermo Jarrell Ash Corp., Franklin, MA, USA). Nitrogen analysis of white flour was performed using the Dumas combustion method at CSBP Soil and Plant Analysis Laboratory (Perth, WA, Australia) and total protein concentration of white flour and bran were

479 determined as: white flour total protein (%) = N concentration x 5.70, and bran total protein (%) = N
480 concentration x 6.31[73].

481 *Quantification of nicotianamine and 2'-deoxymugineic acid*

482 Quantification of 9-fluorenylmethoxycarboxyl chloride (FMOC-Cl) derivatized NA and DMA was
483 performed via RP LC-MS on a 1290 Infinity II and 6490 Triple Quadrupole LC/MS system (Agilent
484 Technologies Inc., Santa Clara, CA) as previously described[30,74]. Briefly, sequential methanol (100%) and
485 deionized H_2O (18MΩ) extractions of pulverized wheat material (25 mg) were combined and derivatized
486 with fresh FMOC-Cl solutions (50 mM, 40 µL). After incubation (60°C, 700 rpm, 15 min), the
487 derivatization reaction was quenched by adding formic acid (FA; pH = 4, 5%, 8.9 µL) and run through a
488 Zorbax Eclipse XDB-C18 Rapid Resolution HS 2.1 x 100 mm, 1.8 µm particle size column (Agilent
489 Technologies Inc.) using aqueous (0.1% v/v FA in dH2O) and organic (0.1% v/v FA in acetonitrile)
490 mobile phases and NA and DMA quantified using a stock calibration set (Toronto Research Chemicals,
491 Toronto, ON, Canada).

492 *In vitro Fe bioavailability bioassay*

493 White flour samples (500 mg) were subjected to the Caco-2 cell bioassay as previously described[30,48,75].
494 Caco-2 cells were maintained in supplemented Dulbecco's modified Eagle medium (DMEM) for 11 days
495 post-seeding and replaced with supplemented minimum essential media (MEM) solution containing less
496 than 80 µg Fe/L at 48 hr prior to the experiment. Gastric-digested samples (1.5 mL) were added to
497 cylindrical Transwell inserts (Corning Life Sciences, Corning, NY) fitted with a semipermeable (15,000
498 Da MWCO) basal membrane (Spectra/Por 2.1, Spectrum Medical, Gardena, CA) and placed within wells
499 containing Caco-2 cell monolayers. After incubation for 2 hr (37 °C) the inserts were removed and
500 additional MEM (1 mL) was added to the cells before incubation for 22 hr (37 °C). Cells were washed
501 twice with a solution (pH = 7.0) containing NaCl (140 mmol/L), KCl (5 mmol/L) and PIPES (10
502 mmol/L), harvested and analysed for ferritin (FER-IRON II Ferritin Assay, Ramco Laboratories,
503 Houston, TX) and total protein contents (Bio-Rad DC Protein Assay, Bio-Rad, Hercules, CA). Caco-2
504 cell ferritin synthesis occurs in response to increases in intracellular Fe and we used the ratio of
505 ferritin/total protein (expressed as ng ferritin/mg protein) as an index of cellular Fe uptake.

506 *Statistical Analysis*

507 Agronomic, grain nutrition, white flour nutrition, and leaf nutrition traits for each environment were
508 analysed using a multi-environment linear mixed model (LMM) that partitioned and accounted for
509 genetic and non-genetic sources of variation. The LMM had the form:

$$\boldsymbol{y} = \boldsymbol{X\tau} + \boldsymbol{Z}_r\boldsymbol{u}_r + \boldsymbol{Z}_C\boldsymbol{u}_C + \boldsymbol{Z}_R\boldsymbol{u}_R + \boldsymbol{\epsilon}$$

and a vector of observed responses across the nine environments had the form: $\boldsymbol{y} = \left(\boldsymbol{y}_1^T ... \boldsymbol{y}_9^T\right)^T$. The vectors of fixed effects ($\boldsymbol{\tau}$) were conformably partitioned to be $\boldsymbol{\tau} = \left[\boldsymbol{\tau}_g^T\, \boldsymbol{\tau}_e^T\, \boldsymbol{\tau}_{eg}^T\right]^T$ where $\boldsymbol{\tau}_g$, and $\boldsymbol{\tau}_e$ were vectors of genotype and environment main effects and $\boldsymbol{\tau}_{eg}$ was a vector of genotype by environment interaction fixed effects, with associated explanatory matrix $\boldsymbol{X} = [\boldsymbol{X}_g\, \boldsymbol{X}_e\, \boldsymbol{X}_{eg}]$. For $i = (r, C, R)$ each of the random effects were also partitioned $\boldsymbol{u}_i = \left[\boldsymbol{u}_{i1}^T ... \boldsymbol{u}_{i9}^T\right]^T$ where $\boldsymbol{u}_i \sim N(\boldsymbol{0}, \oplus_{j=1}^{9}\sigma_{ij}^2\boldsymbol{I})$ and $\oplus$ is the direct sum operator[76] used to indicate block diagonality of the associated variance matrix. Identical to $\boldsymbol{y}$, the multi-environment LMM error term was also conformably partitioned $\boldsymbol{\epsilon} = \left[\boldsymbol{\epsilon}_1^T ... \boldsymbol{\epsilon}_9^T\right]^T$ and assumed to be distributed $\boldsymbol{\epsilon} \sim N(\boldsymbol{0}, \oplus_{j=1}^{9}\sigma_j^2\boldsymbol{I})$. From this full model the genotype (G) x environment (E) interaction was tested and if the interaction was not statistically significant it was removed. The multi-environment model was then refitted with fixed effects $\boldsymbol{\tau}_g$ and $\boldsymbol{\tau}_e$, and eBLUEs for each genotype extracted and compared against NS using a single degree of freedom Wald test. Single and multi-environment linear mixed modelling was computationally conducted using the functionality of the R package ASReml-R[76]. ASReml-R uses the Residual Maximum Likelihood (REML) algorithm[77] for estimation of model parameters and provides a suite of functions for diagnostic assessment of models.

To visualize relationships between traits eBLUEs were extracted from each of the full multi-environment models, compared pairwise using a Pearson correlation and hierarchically clustered. Significant correlations were determined by forming a set of 5,000 permutations of each trait eBLUE, storing the maximum Pearson correlation and calculating p-values based on the number of maximum correlations exceeding the observed pairwise correlation[78]. Hierarchical clustering and graphical visualization of correlation matrices were conducted using the R package corrplot[79]. Other graphs were generated using SigmaPlot v13 (Systat Software Inc., San Jose) software and data are presented as mean ± SEM with biological replicate numbers noted in table and figure legends. Student's *t*-test was used to determine significant differences between means and was conducted using Minitab 17 Statistical software (Minitab, State College, PA).

Data availability statement

All relevant data can be found within the manuscript and its supporting materials.

Acknowledgments

This work was supported by grants from the HarvestPlus program to A.A.T.J and by the Albert Shimmins Fund to J.T.B. We thank Adrian Cox, Leigh Smith, Shahajahan Miyan and Ed Barrett-Lennard at the

Department of Primary Industries and Regional Development Western Australia (Western Australia, Australia) for excellent technical assistance related to CFT components of our research. We also thank Mary Bodis, Yongpei Chang and Shree Giri for their invaluable help provided throughout the project. Analysis of NA and DMA was carried out at Metabolomics Australia (School of BioSciences, The University of Melbourne, Australia), an NCRIS initiative under Bioplatforms Australia Pty Ltd. The authors wish to dedicate this manuscript in memory of Adrian Cox.

Author contributions

Conceptualization, J.T.B., J.P.B., and A.A.T.J.; design, J.T.B., J.P.B., and L.T.M., funding acquisition, J.T.B., and A.A.T.J.; data acquisition and interpretation, J.T.B., J.P.B., L.T.M.M., D.L.C., K.S.H., E.T., R.P.G., R.A., and A.A.T.J.; data analysis, J.T.B., J.P.B., and J.T.; resources, K.S.H., E.T., R.P.G., R.A., and A.A.T.J.; supervision, J.P.B., L.T.M., R.A., and A.A.T.J., visualisation, J.T.B., and J.P.B., writing – original draft, J.T.B.; writing – review and editing, J.T.B., J.P.B., L.T.M.M., D.L.C., K.S.H., E.T., J.T., R.P.G., R.A., and A.A.T.J. All authors have read and approved the final version of the manuscript. All authors agree to be accountable for all aspects of the work in ensuring that questions related to the accuracy or integrity of any part of the work are appropriately investigated and resolved.

Conflict of interest statement

The authors declare no conflict of interest.

Supplementary Material Legends

Figure S1. Replicated plot design of confined field trials at Glenthorne.

Figure S2. Replicated plot design of confined field trials at Katanning and Merredin.

Figure S3. Temperature and rainfall at Glenthorne, Katanning and Merredin.

Figure S4. Multi-trait correlation from multi-environment models of leaf nutrition.

Figure S5. Grain Fe and Zn concentrations (μg / g) in the glasshouse and at Katanning following detillering and leaf removal.

Figure S6. White flour Fe bioavailability at Glenthorne, Katanning and Merredin.

Figure S7. Multi-trait correlation from multi-environment models of agronomic performance, wholemeal flour nutrition and white flour nutrition.

Figure S8. White flour and white bread phytate concentrations (g / 100g).

Table S1. Soil properties at Glenthorne, Katanning and Merredin.

Table S2. Plant trait G x E interactions at Glenthorne, Katanning and Merredin.

Table S3. Tiller number (m^2), biomass (kg ha^{-1}), harvest index (%), and grain number (m^2) at Glenthorne, Katanning and Merredin.

Table S4. Bran Fe, Zn, and P (µg / g) and total protein (%) at Glenthorne, Katanning and Merredin.

Table S5. Wholemeal and white flour P (µg / g) and total protein (%) at Glenthorne, Katanning and Merredin.

Table S6. Wholemeal flour Ca, Cu, K, Mg, Mn, and S (µg / g) at Glenthorne, Katanning and Merredin.

Table S7. White flour Ca, Cu, K, Mg, Mn, and S (µg / g) at Glenthorne, Katanning and Merredin.

Table S8. Bran Ca, Cu, K, Mg, Mn, and S (µg / g) at Glenthorne, Katanning and Merredin.

Table S9. Leaf Fe, Zn, and P (µg / g) at Glenthorne, Katanning and Merredin.

Table S10. Flag leaf Ca, Cu, K, Mg, Mn, and S (µg / g) at Glenthorne, Katanning and Merredin.

Table S11. Leaf Ca, Cu, K, Mg, Mn, and S (µg / g) at Glenthorne, Katanning and Merredin.

References

1. Shewry, P. Wheat. *J. Exp. Bot.* **60**, 1537–1553 (2009).

2. Shewry, P. R. & Hey, S. J. The contribution of wheat to human diet and health. *Food Energy Secur.* **4**, 178–202 (2015).

3. Beal, T., Massiot, E., Arsenault, J. E., Smith, M. R. & Hijmans, R. J. Global trends in dietary micronutrient supplies and estimated prevalence of inadequate intakes. *PLoS One* **12**, e0175554 (2017).

4. Lopez, A., Cacoub, P., Macdougall, I. C. & Peyrin-Biroulet, L. Iron deficiency anaemia. *Lancet* **387**, 907–916 (2016).

5. Bouis, H. E., Hotz, C., McClafferty, B., Meenakshi, J. V. & Pfeiffer, W. H. Biofortification: A new tool to reduce micronutrient malnutrition. *Food Nutr. Bull.* **32**, S31-40 (2011).

6. Appels, R. *et al.* Shifting the limits in wheat research and breeding using a fully annotated reference genome. *Science (80-.).* **361**, 1–13 (2018).

7. Listman, G. M. *et al.* Improving Nutrition through Biofortification: Preharvest and Postharvest Technologies. *Cereal Foods World* **64**, 1–7 (2019).

8. Welch, R. M. & Graham, R. D. Breeding for micronutrients in staple food crops from a human nutrition perspective. *J. Exp. Bot.* **55**, 353–364 (2004).

9. Velu, G., Ortiz-Monasterio, I., Cakmak, I., Hao, Y. & Singh, R. P. Biofortification strategies to increase grain zinc and iron concentrations in wheat. *J. Cereal Sci.* **59**, 365–372 (2014).

10. White, P. J. & Broadley, M. R. Biofortification of crops with seven mineral elements often lacking in human diets - Iron, zinc, copper, calcium, magnesium, selenium and iodine. *New Phytol.* **182**, 49–84 (2009).

11. Tabbita, F., Pearce, S. & Barneix, A. J. Breeding for increased grain protein and micronutrient content in wheat: Ten years of the GPC-B1 gene. *J. Cereal Sci.* **73**, 183–191 (2017).

12. Cakmak, I., Pfeiffer, W. H. & McClafferty, B. Biofortification of Durum Wheat with Zinc and Iron. *Cereal Chem.* **87**, 10–20 (2010).

13. Velu, G. *et al.* Genetic dissection of grain zinc concentration in spring wheat for mainstreaming biofortification in CIMMYT wheat breeding. *Sci. Rep.* **8**, 1–10 (2018).

14. Velu, G. *et al.* Assessing Genetic Diversity to Breed Competitive Biofortified Wheat With Enhanced Grain Zn and Fe Concentrations. *Front. Plant Sci.* **9**, 1–11 (2019).

15. Velu, G. *et al.* Performance of biofortified spring wheat genotypes in target environments for grain zinc and iron concentrations. *F. Crop. Res.* **137**, 261–267 (2012).

16. Distelfeld, A., Avni, R. & Fischer, A. M. Senescence, nutrient remobilization, and yield in wheat and barley. *J. Exp. Bot.* **65**, 3783–3798 (2014).

17. Borrill, P. *et al.* Biofortification of wheat grain with iron and zinc: integrating novel genomic resources and knowledge from model crops. *Front. Plant Sci.* **5**, 1–8 (2014).

18. Uauy, C., Distelfeld, A., Fahima, T., Blechl, A. & Dubcovsky, J. A NAC Gene regulating senescence improves grain protein, zinc, and iron content in wheat. *Science (80-.).* **314**, 1298–1301 (2006).

19. Velu, G. *et al.* Characterization of grain protein content gene (GPC-B1) introgression lines and its potential use in breeding for enhanced grain zinc and iron concentration in spring wheat. *Acta Physiol. Plant.* **39**, 1–9 (2017).

20. Distelfeld, A. *et al.* Multiple QTL-effects of wheat Gpc-B1 locus on grain protein and micronutrient concentrations. *Physiol. Plant.* **129**, 635–643 (2007).

21. Mattila, P., Pihlava, J. M. & Hellström, J. Contents of phenolic acids, alkyl- and alkenylresorcinols, and avenanthramides in commercial grain products. *J. Agric. Food Chem.* **53**, 8290–8295 (2005).

22. Chvátalová, K., Slaninová, I., Březinová, L. & Slanina, J. Influence of dietary phenolic acids on redox status of iron: Ferrous iron autoxidation and ferric iron reduction. *Food Chem.* **106**, 650–660 (2008).

23. Gillooly, M. *et al.* The effects of organic acids, phytates and polyphenols on the absorption of iron from vegetables. *Br. J. Nutr.* **49**, 331 (1983).

24. Schlemmer, U., Frølich, W., Prieto, R. M. & Grases, F. Phytate in foods and significance for humans: Food sources, intake, processing, bioavailability, protective role and analysis. *Mol. Nutr. Food Res.* **53**, 330–375 (2009).

25. Tang, J. *et al.* Mineral element distributions in milling fractions of Chinese wheats. *J. Cereal Sci.* **48**, 821–828 (2008).

26. Singh, S. P. *et al.* Pattern of iron distribution in maternal and filial tissues in wheat grains with contrasting levels of iron. *J. Exp. Bot.* **64**, 3249–60 (2013).

27. Balk, J. *et al.* Improving wheat as a source of iron and zinc for global nutrition. *Nutr. Bull.* **44**, 53–59 (2019).

28. De Brier, N. *et al.* Element distribution and iron speciation in mature wheat grains (*Triticum aestivum* L.) using synchrotron X-ray fluorescence microscopy mapping and X-ray absorption near-edge structure (XANES) imaging. *Plant. Cell Environ.* **39**, 1835–1847 (2016).

29. Moore, K. L. *et al.* Localisation of iron in wheat grain using high resolution secondary ion mass spectrometry. *J. Cereal Sci.* **55**, 183–187 (2012).

30. Beasley, J. T. *et al.* Metabolic engineering of bread wheat improves grain iron concentration and

bioavailability. *Plant Biotechnol. J.* 1–13 (2019). doi:10.1111/pbi.13074

31. Glass, S. & Fanzo, J. Genetic modification technology for nutrition and improving diets: an ethical perspective. *Curr. Opin. Biotechnol.* **44**, 46–51 (2017).

32. Olsen, L. I. *et al.* Mother-plant-mediated pumping of zinc into the developing seed. *Nat. Plants* **2**, 1–6 (2016).

33. Stomph, T. J., Choi, E. Y. & Stangoulis, J. C. R. Temporal dynamics in wheat grain zinc distribution: Is sink limitation the key? *Ann. Bot.* **107**, 927–937 (2011).

34. Maillard, A. *et al.* Leaf mineral nutrient remobilization during leaf senescence and modulation by nutrient deficiency. *Front. Plant Sci.* **6**, 1–15 (2015).

35. Pottier, M., Masclaux-Daubresse, C., Yoshimoto, K. & Thomine, S. Autophagy as a possible mechanism for micronutrient remobilization from leaves to seeds. *Front Plant Sci* **5**, 11 (2014).

36. Waters, B. M., Uauy, C., Dubcovsky, J. & Grusak, M. A. Wheat (Triticum aestivum) NAM proteins regulate the translocation of iron, zinc, and nitrogen compounds from vegetative tissues to grain. *J. Exp. Bot.* **60**, 4263–4274 (2009).

37. Zielińska-Dawidziak, M. Plant ferritin—a source of iron to prevent its deficiency. *Nutrients* **7**, 1184–1201 (2015).

38. Kim, S. A. *et al.* Localization of Iron in Arabidopsis Seed Requires the Vacuolar Membrane Transporter VIT1. *Science (80-.).* **314**, 1295–1298 (2006).

39. Zhang, Y., Xu, Y. H., Yi, H. Y. & Gong, J. M. Vacuolar membrane transporters OsVIT1 and OsVIT2 modulate iron translocation between flag leaves and seeds in rice. *Plant J.* **72**, 400–410 (2012).

40. Connorton, J. M. *et al.* Wheat Vacuolar Iron Transporter TaVIT2 Transports Fe and Mn and Is Effective for Biofortification. *Plant Physiol.* **174**, 2434–2444 (2017).

41. Connorton, J. M., Balk, J. & Rodríguez-Celma, J. Iron homeostasis in plants-a brief overview. *Metallomics* **9**, 813–823 (2017).

42. Andresen, E., Peiter, E. & Küpper, H. Trace metal metabolism in plants. *J. Exp. Bot.* **69**, 909–954 (2018).

675 43. Takahashi, M. *et al.* Role of nicotianamine in the intracellular delivery of metals and plant
676 reproductive development. *Plant Cell* **15**, 1263–80 (2003).

677 44. Kobayashi, T., Nozoye, T. & Nishizawa, N. K. Iron transport and its regulation in plants. *Free*
678 *Radic. Biol. Med.* **133**, 11–20 (2018).

679 45. Oburger, E. *et al.* Root exudation of phytosiderophores from soil-grown wheat. *New Phytol.*
680 (2014). doi:10.1111/nph.12868

681 46. Eagling, T. *et al.* Distribution and Speciation of Iron and Zinc in Grain of Two Wheat Genotypes.
682 *J. Agric. Food Chem.* **62**, 708–716 (2014).

683 47. Singh, S. P., Keller, B., Gruissem, W. & Bhullar, N. K. Rice NICOTIANAMINE SYNTHASE 2
684 expression improves dietary iron and zinc levels in wheat. *Theor. Appl. Genet.* **130**, 283–292
685 (2017).

686 48. Trijatmiko, K. R. *et al.* Biofortified indica rice attains iron and zinc nutrition dietary targets in the
687 field. *Sci. Rep.* **6**, 1–13 (2016).

688 49. Bouis, H. E. & Saltzman, A. Improving nutrition through biofortification: A review of evidence
689 from HarvestPlus, 2003 through 2016. *Glob. Food Sec.* **12**, 49–58 (2017).

690 50. Dubois, M., Van den Broeck, L. & Inzé, D. The Pivotal Role of Ethylene in Plant Growth. *Trends*
691 *Plant Sci.* **23**, 311–323 (2018).

692 51. Habben, J. E. *et al.* Transgenic alteration of ethylene biosynthesis increases grain yield in maize
693 under field drought-stress conditions. *Plant Biotechnol. J.* **12**, 685–693 (2014).

694 52. Ambavaram, M. M. R. *et al.* Coordinated regulation of photosynthesis in rice increases yield and
695 tolerance to environmental stress. *Nat. Commun.* **5**, 1–14 (2014).

696 53. Larkin, P. J. & Scowcroft, W. R. Somaclonal variation - a novel source of variability from cell
697 cultures for plant improvement. *Theor. Appl. Genet.* **60**, 197–214 (1981).

698 54. Bregitzer, P., Halbert, S. E. & Lemaux, P. G. Somaclonal variation in the progeny of transgenic
699 barley. *Theor. Appl. Genet.* **96**, 421–425 (1998).

700 55. Banakar, R. *et al.* Phytosiderophores determine thresholds for iron and zinc accumulation in
701 biofortified rice endosperm while inhibiting the accumulation of cadmium. *J. Exp. Bot.* **68**, 4983–
702 4995 (2017).

703 56. Morrissey, J. & Guerinot, M. Lou. Iron Uptake and Transport in Plants. *Plant Membr. Vacuolar*
704 *Transp.* **109**, 149–172 (2009).

705 57. Broadley, M. R., White, P. J., Hammond, J. P., Zelko, I. & Lux, A. Zinc in plants. *New Phytol.*
706 **173**, 677–702 (2007).

707 58. Campbell, G. M. Chapter 7 - Roller Milling of Wheat. *Handb. Powder Technol.* **12**, 391–425
708 (2007).

709 59. Beasley, J. T., Hart, J. J., Tako, E., Glahn, R. P. & Johnson, A. A. T. Investigation of
710 Nicotianamine and 2' Deoxymugineic Acid as Enhancers of Iron Bioavailability in Caco-2 cells.
711 *Nutrients* **11**, 1–12 (2019).

712 60. Martin, C. & Li, J. Medicine is not health care, food is health care: plant metabolic engineering,
713 diet and human health. *New Phytol.* **216**, 699–719 (2017).

714 61. Nozoye, T. The Nicotianamine Synthase Gene Is a Useful Candidate for Improving the Nutritional
715 Qualities and Fe-Deficiency Tolerance of Various Crops. *Front. Plant Sci.* **9**, 1–7 (2018).

716 62. Knez, M. *et al.* Linoleic Acid:Dihomo-γ-Linolenic Acid Ratio Predicts the Efficacy of Zn-
717 Biofortified Wheat in Chicken (Gallus gallus). *J. Agric. Food Chem.* **66**, 1394–1400 (2018).

718 63. Shewry, P. R. & Tatham, A. S. Disulphide bonds in wheat gluten proteins. *J. Cereal Sci.* **25**, 207–
719 227 (1997).

720 64. Luo, C., Branlard, G., Griffin, W. B. & McNeil, D. L. The effect of nitrogen and sulphur
721 fertilisation and their interaction with genotype on wheat glutenins and quality parameters. *J.*
722 *Cereal Sci.* **31**, 185–194 (2000).

723 65. Tsednee, M., Huang, Y. C., Chen, Y. R. & Yeh, K. C. Identification of metal species by ESI-
724 MS/MS through release of free metals from the corresponding metal-ligand complexes. *Sci. Rep.*
725 **6**, 1–13 (2016).

726 66. Mason, S. D., McLaughlin, M. J., Johnston, C. & McNeill, A. Soil test measures of available P
727 (Colwell, resin and DGT) compared with plant P uptake using isotope dilution. *Plant Soil* **373**,
728 711–722 (2013).

729 67. Zhang, Y. *et al.* Comparison of soil analytical methods for estimating wheat potassium fertilizer
730 requirements in response to contrasting plant K demand in the glasshouse. *Sci. Rep.* **7**, 1–10

(2017).

68. Lindsay, W. L. & Norvell, W. A. Development of a DTPA Soil Test for Zinc, Iron, Manganese, and Copper. *Soil Sci. Soc. Am. J.* **42**, 421–428 (1978).

69. Gupta, S. *et al.* Spatio-Temporal Metabolite and Elemental Profiling of Salt Stressed Barley Seeds During Initial Stages of Germination by MALDI-MSI and μ-XRF Spectrometry. *Front. Plant Sci.* **10**, 1–17 (2019).

70. Winters, M. *et al.* Defined co-cultures of yeast and bacteria modify the aroma, crumb and sensory properties of bread. *J. Appl. Microbiol.* **127**, 778–793 (2019).

71. Rodriguez-Ramiro, I. *et al.* Assessment of iron bioavailability from different bread making processes using an in vitro intestinal cell model. *Food Chem.* **228**, 91–98 (2017).

72. Dias, D. M. *et al.* Iron Biofortified Carioca Bean (Phaseolus vulgaris L.) — Based Brazilian Diet Delivers More Absorbable Iron and Affects the Gut Microbiota In Vivo (Gallus gallus). *Nutrients* **10**, 1–20 (2018).

73. WHO/FAO. Food energy – methods of analysis. *FAO Food Nutr. Pap.* 93 (2002). doi:ISSN 0254-4725

74. Selby-Pham, J. *et al.* Diurnal Changes in Transcript and Metabolite Levels during the Iron Deficiency Response of Rice. *Rice* **10**, 1–15 (2017).

75. Glahn, R. P., Lee, O. A., Yeung, A., Goldman, M. I. & Miller, D. D. Caco-2 cell ferritin formation predicts nonradiolabeled food iron availability in an in vitro digestion/Caco-2 cell culture model. *J. Nutr.* **128**, 1555–61 (1998).

76. Butler, D. G., Cullis, B. R., Gilmour, A. R., Gogel, B. J. & Thompson, R. *ASReml-R Reference Manual Version 4*. *VSN International Ltd* (VSN International Ltd, 2018).

77. Patterson, H. D. & Thompson, R. Recovery of inter-block information when block sizes are unequal. *Biometrika* **58**, 545–554 (1971).

78. Hill, C. B. *et al.* Detection of QTL for metabolic and agronomic traits in wheat with adjustments for variation at genetic loci that affect plant phenology. *Plant Sci.* **233**, 143–154 (2015).

79. Wei, T. & Simko, V. R package 'corrplot': Visualization of a Correlation Matrix (Version 0.84). (2017). Available at: https://github.com/taiyun/corrplot.

Figure/Table Legends

Figure 1. Agronomic performance of bread wheat constitutively expressing the rice nicotianamine synthase 2 (*OsNAS2*) gene (CE-1.1, CE-1.2, and CE-1.3) alongside the null segregant and cv. Mace over three field seasons at Glenthorne. **a**) Schematic representation of the T-DNA construct. RB and LB: right and left borders, respectively; UBI-1: maize ubiquitin 1 promoter; *OsNAS2*: rice nicotianamine synthase 2 gene (LOC_Os03 g19420); NOS: nopaline synthase terminator; 2 x 35S: dual promoter of 35S cauliflower mosaic virus gene; hyg: hygromycin phosphotransferase gene; 35S: terminator of 35S cauliflower mosaic virus gene. **b**) an image of replicated plots at Glenthorne during the 2017 field season. **c**) Soil pH (green circles), as well as soil Fe (red bars) and Zn (dark grey bars) concentrations (mg / Kg) are provided for the three field seasons. **d-j**) Bars indicate best linear unbiased estimators of the null segregant (light grey), CE-1.1 (light brown), CE-1.2 (orange), CE-1.3 (dark brown), and Mace (black) for **d**) plant height (cm), **e**) thousand grain weight (g), **f**) grain yield (kg ha^{-1}) and the concentrations of **g**) Fe (µg / g), **h**) Zn (µg / g), **i**) NA (µmol / g), and **j**) DMA (µmol / g) in wholemeal flour (left panel) and white flour (right panel). A minimum of three replicates per genotype were included for each field season and asterisks represent significant differences to the NS for $p < 0.05$ (*), $p \leq 0.01$ (**), $p \leq 0.001$ (***) as determined by Wald test. n.a = not applicable.

Figure 2. Agronomic performance, wholemeal and white flour nutritional composition of null segregant, CE-1.1, CE-1.2, CE-1.3 and Mace over three field seasons at Katanning. **a**) An image of 18m^2 replicated plots for the 2017 field season is provided. **b**) Soil pH (green circles), as well as soil Fe (red bars) and Zn (dark grey bars) concentrations (mg / Kg) are provided for the three field seasons. **c-i**) Bars indicate best linear unbiased estimators of the null segregant (light grey), CE-1.1 (light brown), CE-1.2 (orange), CE-1.3 (dark brown), and Mace (black) for **c**) plant height (cm), **d**) thousand grain weight (g), **e**) grain yield (kg ha^{-1}) and the concentrations of **f**) Fe (µg / g), **g**) Zn (µg / g), **h**) NA (µmol / g), and **i**) DMA (µmol / g) in wholemeal flour (left panel) and white flour (right panel). A minimum of three replicates per genotype were included for each field season and asterisks represent significant differences to the NS for $p < 0.05$ (*), $p \leq 0.01$ (**), $p \leq 0.001$ (***) as determined by Wald test. n.a = not applicable.

Figure 3. Agronomic performance, wholemeal and white flour nutritional composition of null segregant, CE-1.1, CE-1.2, CE-1.3 and Mace over three field seasons at Merredin. **a**) An image of 18m^2 replicated plots for the 2017 field season is provided. **b**) Soil pH (green circles), as well as soil Fe (red bars) and Zn (dark grey bars) concentrations (mg / Kg) are provided for the three field seasons. **c-i**) Bars indicate best linear unbiased estimators of the null segregant (light grey), CE-1.1 (light brown), CE-1.2 (orange), CE-1.3 (dark brown), and Mace (black) for **c**) plant height (cm), **d**) thousand grain weight (g), **e**) grain yield

(kg ha^{-1}) and the concentrations of **f**) Fe (µg / g), **g**) Zn (µg / g), **h**) NA (µmol / g), and **i**) DMA (µmol / g) in wholemeal flour (left panel) and white flour (right panel). A minimum of three replicates per genotype were included for each field season and asterisks represent significant differences to the NS for $p < 0.05$ (*), $p \leq 0.01$ (**), $p \leq 0.001$ (***) as determined by Wald test. n.a = not applicable.

Figure 4. Multi-trait correlation of empirical best linear unbiased estimators (eBLUEs) obtained from the multi-environment models of agronomic performance, grain nutrition and white flour nutrition of NS, CE-1 and Mace. Agronomic performance variables include grain yield (YLD), harvest index (HI), thousand grain weight (TGW), total biomass (BIO), tiller number per m^2 (TN.m2), grain number per m^2 (GN.m2), plant height (HGT). Wholemeal (WG) and white flour (WF) nutrition variables include Fe, Zn, P, NA, and DMA concentrations, total protein (Pro) and Caco-2 cell ferritin production (Fer). Each circle represents a positive (blue) or negative (red) pairwise Pearson correlation coefficient between variables, with the diameter of the circle proportional to the absolute value. Asterisks denote significant correlations for $p < 0.05$ (*), $p \leq 0.01$ (**), $p \leq 0.001$ (***).

Figure 5. White bread nutritional composition of NS and CE-1 sibling lines at Glenthorne, Katanning and Merredin. Bars indicate best linear unbiased estimators for the concentrations of **a**) Fe (µg / g), **b**) Zn (µg / g), **c**) NA (µmol / g), and **d**) DMA (µmol / g) at each field site in 2016. Three replicates per genotype were included in the analysis and asterisks represent significant differences to the NS for $p < 0.05$ (*), $p \leq 0.01$ (**), $p \leq 0.001$ (***) as determined by Wald test. Photos show representative cross sections of NS and CE-1 loaves from Katanning prior to analysis. Scale bar = 1cm.

Table 1. The concentrations of Fe (µg / g), Zn (µg / g), NA (µmol / g), DMA (µmol / g), and phytate (mg / g) in null segregant (NS) and CE-1 grain fractions at Merredin in 2017. Values represent mean ± SEM of three biological replicates with three technical replicates for Fe and Zn, four biological replicates for NA and DMA, and two biological replicates with three technical replicates for phytate. Asterisks denote significant differences for $p < 0.05$ (*), $p \leq 0.01$ (**), $p \leq 0.001$ (***) as determined by Student's t-test.

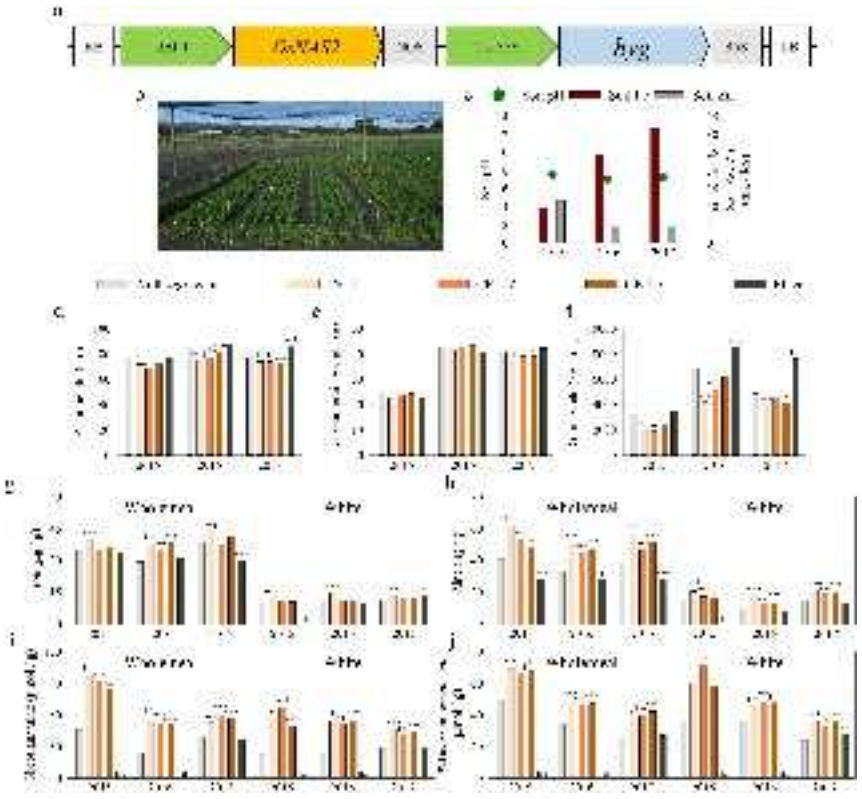

tpj_15623_f1.jpg

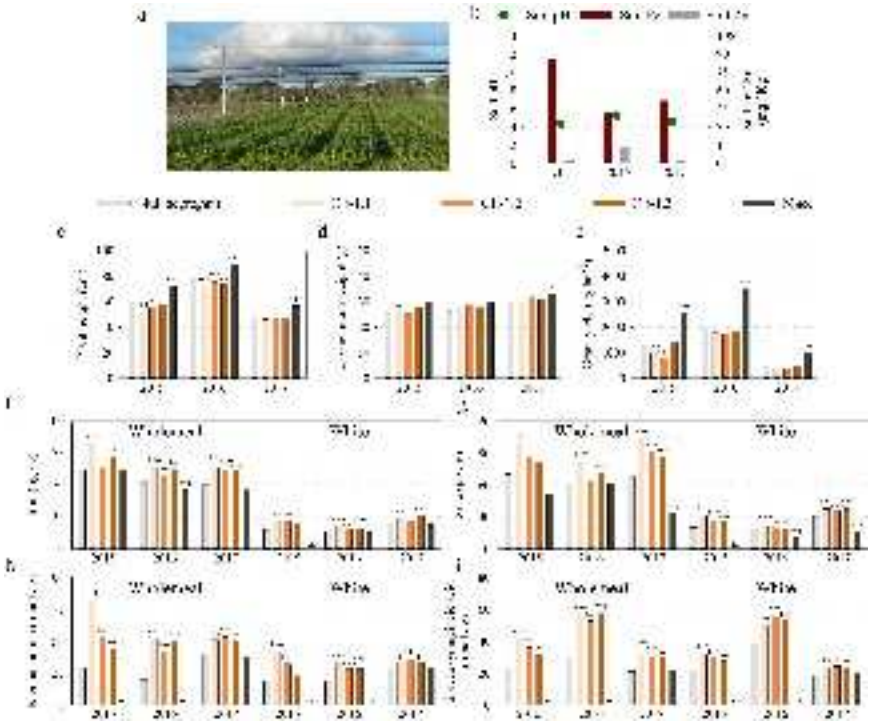

tpj_15623_f2.jpg

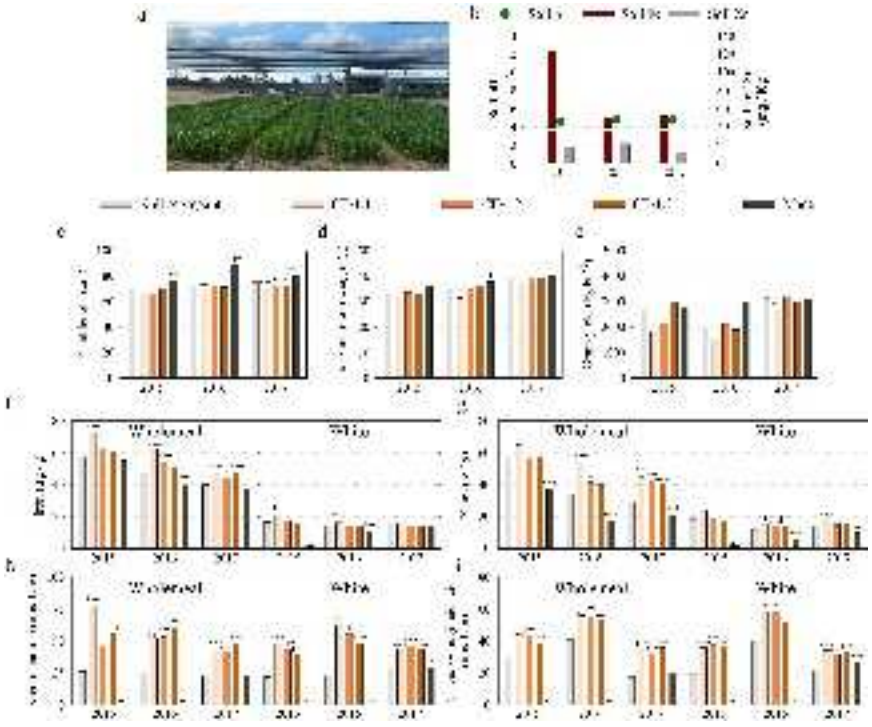

tpj_15623_f3.jpg

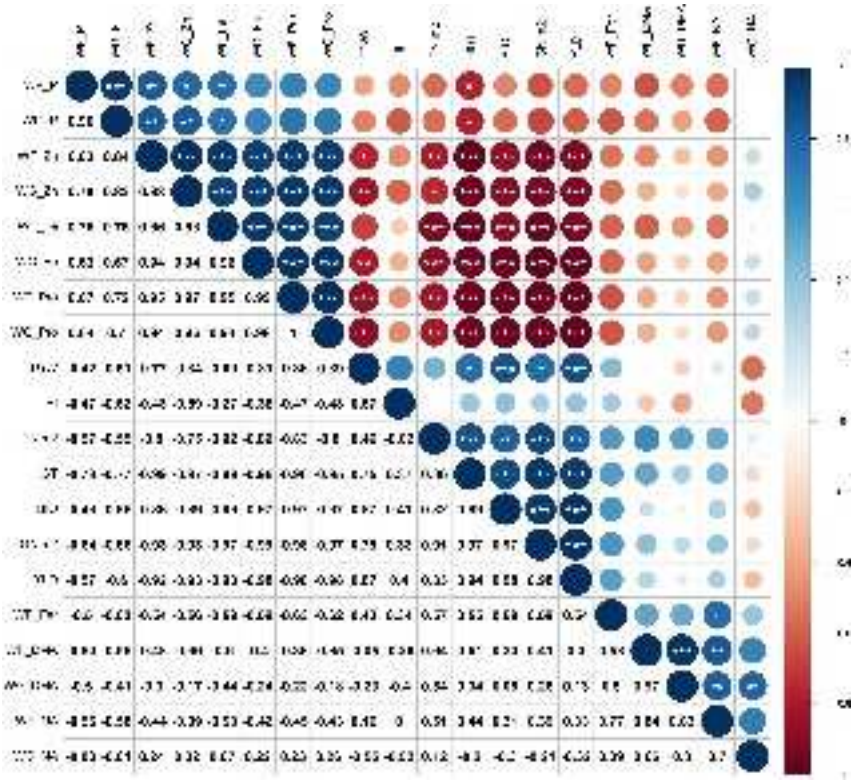

tpj_15623_f4.jpg

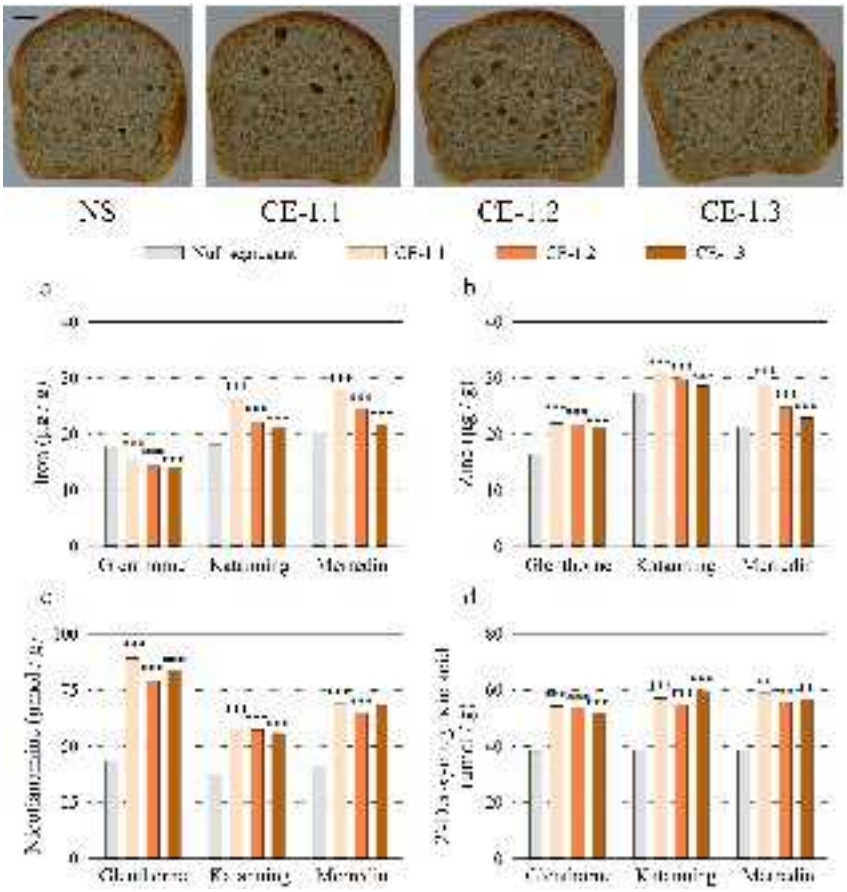

tpj_15623_f5.jpg